



HAL
open science

Harmful *Ostreopsis cf. ovata* blooms could extend in time span with climate change in the Western Mediterranean Sea

Salomé Fabri-Ruiz, Elisa Berdalet, Caroline Ulses, Samuel Somot, M. Vila, Rodolphe Lemee, Jean-Olivier Irisson

► To cite this version:

Salomé Fabri-Ruiz, Elisa Berdalet, Caroline Ulses, Samuel Somot, M. Vila, et al.. Harmful *Ostreopsis cf. ovata* blooms could extend in time span with climate change in the Western Mediterranean Sea. *Science of the Total Environment*, 2024, 947, pp.174726. 10.1016/j.scitotenv.2024.174726. hal-04652166

HAL Id: hal-04652166

<https://hal.science/hal-04652166v1>

Submitted on 18 Jul 2024

HAL is a multi-disciplinary open access archive for the deposit and dissemination of scientific research documents, whether they are published or not. The documents may come from teaching and research institutions in France or abroad, or from public or private research centers.

L'archive ouverte pluridisciplinaire **HAL**, est destinée au dépôt et à la diffusion de documents scientifiques de niveau recherche, publiés ou non, émanant des établissements d'enseignement et de recherche français ou étrangers, des laboratoires publics ou privés.



Distributed under a Creative Commons Attribution 4.0 International License



Harmful *Ostreopsis* cf. *ovata* blooms could extend in time span with climate change in the Western Mediterranean Sea

S. Fabri-Ruiz^{a,b,*}, E. Berdalet^c, C. Ulses^d, S. Somot^e, M. Vila^c, R. Lemée^a, J.-O. Irisson^a

^a Sorbonne Université, CNRS, Laboratoire d'Océanographie de Villefranche, Villefranche-sur-Mer, France

^b DECOD, L'Institut Agro, IFREMER, INRAE, 44000 Nantes, France

^c Institute of Marine Sciences (ICM-CSIC), Barcelona, Spain

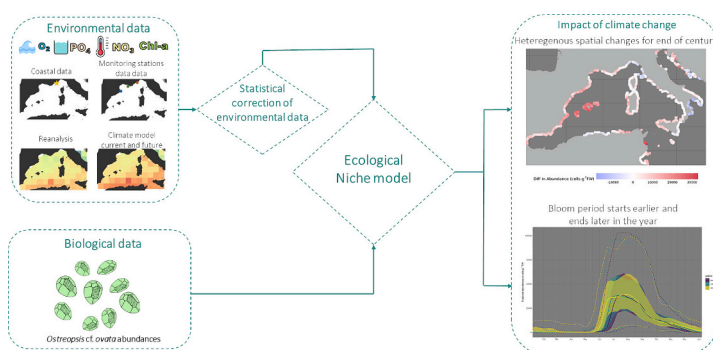
^d Laboratoire d'Etudes en Géophysique et Océanographie Spatiales (LEGOS), Université de Toulouse, CNES, CNRS, IRD, UT3, Toulouse, France

^e CNRM, Université de Toulouse, Météo-France, CNRS, Toulouse, France

HIGHLIGHTS

- Climate change impacts on *O. cf. ovata* dynamics in the Mediterranean is investigated.
- Temporal changes in T° and chlorophyll are the best predictors of abundance.
- In the future, *O. cf. ovata* blooms could start earlier and finish later in the year.
- *O. cf. ovata* abundances are expected to rise on the French, Spanish, and Adriatic coasts.
- These changes may negatively affect ecosystems, health, and the economy.

GRAPHICAL ABSTRACT



ARTICLE INFO

Editor: Ashantha Goonetilleke

Keywords:

Ecological habitat model
Climate change
Harmful algal bloom
Seawater temperature
CDF-t

ABSTRACT

Fast environmental changes and high coastal human pressures and impacts threaten the Mediterranean Sea. Over the last decade, recurrent blooms of the harmful dinoflagellate *Ostreopsis* cf. *ovata* have been recorded in many Mediterranean beaches. These microalgae produce toxins that affect marine organisms and human health. Understanding the environmental conditions that influence the appearance and magnitude of *O. cf. ovata* blooms, as well as how climate change will modify its future distribution and dynamics, is crucial for predicting and managing their effects. This study investigates whether the spatio-temporal distribution of this microalga and the frequency of its blooms could be altered in future climate change scenarios in the Mediterranean Western basin. For the first time, an ecological habitat model (EHM) is forced by physico-chemical climate change simulations at high-resolution, under the strong greenhouse gas emission trajectory (RCP8.5). It allows to characterize how *O. cf. ovata* may respond to projected conditions and how its distribution could shift over a wide spatial scale, in this plausible future. Before being applied to the EHM, future climate simulations are further refined by using a statistical adaptation method (Cumulative Distribution Function transform) to improve the predictions robustness. Temperature (optimum 23–26 °C), high salinity (>38 psu) and high inorganic nutrient concentrations (nitrate >0.25 mmol N·m⁻³ and phosphate >0.035 mmol P·m⁻³) drive *O. cf. ovata* abundances. High spatial disparities in future abundances are observed. Namely, *O. cf. ovata* abundances could increase on the

* Corresponding author at: Sorbonne Université, CNRS, Laboratoire d'Océanographie de Villefranche, Villefranche-sur-Mer, France.

E-mail address: salome.fabri.ruiz@ifremer.fr (S. Fabri-Ruiz).

<https://doi.org/10.1016/j.scitotenv.2024.174726>

Received 8 March 2024; Received in revised form 9 July 2024; Accepted 10 July 2024

Available online 11 July 2024

0048-9697/© 2024 The Author(s). Published by Elsevier B.V. This is an open access article under the CC BY license (<http://creativecommons.org/licenses/by/4.0/>).

Mediterranean coasts of France, Spain and the Adriatic Sea while a decrease is expected in the Tyrrhenian Sea. The bloom period could be extended, starting earlier and continuing later in the year. From a methodological point of view, this study highlights best practices of EHMs in the context of climate change to identify sensitive areas for current and future harmful algal blooms.

1. Introduction

Climate change is unequivocal and results from an unprecedented rise in anthropogenic greenhouse gas concentrations (IPCC, 2023). Its impacts are global and pervasive, including changes in seawater physico-chemical properties (temperature, salinity, stratification, pH) and ocean biogeochemistry (essential nutrients and carbon dynamics; Doney et al., 2012; Gattuso et al., 2015; Hoegh-Guldberg and Bruno, 2010). Thus, in the Mediterranean Sea, under the RCP8.5 scenario assumption that CO₂ emissions continue to increase, the average sea surface temperature (SST) is projected to increase by 2.7 to 3.8 °C at the end of this century, compared to the end of the 20th century (Darmaraki et al., 2019). For the same RCP8.5 scenario, coupled regional climate change simulations also show a decrease in surface-layer salinity in the Western basin, with anomalies ranging from -0.42 to -0.01 (Soto-Navarro et al., 2020). These physico-chemical changes are expected to have a profound effect on marine ecosystems functioning and to alter the historical biogeographic distribution of some marine species (Burrows et al., 2011; Edwards and Richardson, 2004; Moullec et al., 2019; Poloczanska et al., 2013; Wittmann and Pörtner, 2013).

Coastal regions represent a small fraction of the world's ocean but are of considerable socio-economic importance because they provide many ecosystem goods and services to humans. It is estimated that 2.15 billion people of the world live in the near-coastal zone (Reimann et al., 2023). Harmful Algal Blooms (HABs) occurring in coastal ecosystems have received a lot of attention from researchers and stakeholders, because of their significant negative consequences on human health, food safety, the economy and marine ecosystems (Erdner et al., 2008; Kouakou and Poder, 2019). HABs were estimated to cause an annual loss to the European Union of ca. 1 billion dollars (Hoagland and Scatista, 2006). For various types of aquaculture facilities, single HAB events have been shown to result in losses in the hundreds of millions (Trainer, 2020). The possibility that climate change may increase certain HABs' frequency and intensity and widen their seasonal occurrence window and geographical distribution, is a matter of debate and concern among the scientific community and stakeholders. It is stimulating research in this direction (Anderson et al., 2012; Berdalet et al., 2017; Gilbert et al., 2014; Gobler et al., 2017; Moore et al., 2008; Tester et al., 2020).

In the Mediterranean Sea, *Ostreopsis cf. ovata* (Fukuyo, 1981), a benthic dinoflagellate that can be toxic, has become common, regularly blooming in summer. Massive abundances have been well documented along the coasts of Spain, Italy, France, Algeria, Croatia, etc. (e.g., Carnicer et al., 2015; Cochu et al., 2013; Mangialajo et al., 2011, 2008; Ninčević Gladan et al., 2019; Vila et al., 2001). Predominantly epiphytic (on macroalgae and seagrass), cells are also found on abiotic substrates (sediment, rocks or pebbles; Accoroni and Totti, 2016; Cochu et al., 2013; Gémin et al., 2020; Meroni et al., 2018; Vila et al., 2001). Cells also detach from this benthic habitat due to water motion and/or internal cell rhythms (Ciminiello et al., 2014; Pavaux et al., 2021, 2020). *Ostreopsis cf. ovata* blooms likely affect people, via direct contact with cells floating in the seawater and inhalation of aerosols created at the air-sea interface. *Ostreopsis cf. ovata* blooms have been associated with acute (but mild) respiratory irritation, general malaise, headache, low fever, eye irritation and dermatitis (Berdalet et al., 2022; Durando et al., 2007; Gallitelli et al., 2005; Paradis et al., 2024; Pfannkuchen et al., 2012; Tichadou et al., 2010; Vila et al., 2016). Toxic effects on marine organisms, such as copepods, sea urchins, jellyfish, and mussels, have also been reported (Faimali et al., 2012; Gorbi et al., 2013; Guidi-Guilvard et al., 2012; Neves et al., 2018; Pavaux et al., 2020). These health

and ecological impacts have been attributed to palytoxin analogues (ovatoxins, putative palytoxin) produced by these microalgae, although the direct cause-effect link has not yet been fully established (Tubaro et al., 2011). While this microalgae socio-economic cost has not yet been estimated across the European Union, several studies agree that *Ostreopsis* spp. blooms could have a significant impact, particularly affecting the beach visitors' activities and the tourism industry (Berdalet et al., 2022, 2017). The factors influencing the dynamics of *Ostreopsis* bloom must be understood in this context. Information on *O. cf. ovata* bloom proliferation is inferred, in part, from laboratory studies aiming to define the optimal growth conditions of different strains from the Mediterranean Sea (Carnicer et al., 2016; Granéli et al., 2011; Scalco et al., 2012) or from other regions (reviewed by Tester et al., 2020). A few studies, mainly focused on local scales (near the Ebro Delta, on the French Riviera, on beaches around Monaco), have attempted to determine which environmental variables drive in situ seasonal patterns and how these variables affect cell dynamics (Carnicer et al., 2015; Cochu et al., 2013, 2011). A meta-analysis has examined those questions at the scale of the north-western Mediterranean Sea with three-year data from the beginning of the 21st century (Mangialajo et al., 2011). Still, no systematic study has explored the distribution patterns over large temporal (decades) or spatial (whole basin) scales. The relationship with environmental conditions at those scales is therefore also unknown. The consequences for *O. cf. ovata* blooms of shifts in those conditions due to climate change have not been assessed either. In the context of ongoing climate change, particularly in the Mediterranean region (Giorgi, 2006), and the uncertainties about this benthic taxon's potential increase (e.g. Zingone et al., 2021), such a study is necessary. Indeed, forecasting shifts in species distribution patterns in response to climate change is needed to better understand and mitigate their harmful effects on human populations and marine ecosystems. Modeling is one of the only tools available to turn historical observations into such future predictions (Araújo and Guisan, 2006; Benedetti et al., 2018; Melo-Merino et al., 2020; Robinson et al., 2011, 2017).

Ecological Habitat Models (EHMs) are an effective approach to predict biogeographic patterns of target species (Elith and Leathwick, 2009; Guisan and Thuiller, 2005; Robinson et al., 2011). EHMs quantify the relationships between the presence (concentration) of species and environment variables through a correlative statistical framework, to define the species' environmental habitat (Elith et al., 2008; Guisan and Zimmermann, 2000; Peterson et al., 2015; Soberon and Peterson, 2005). After assessing this relationship's robustness, the model can be projected in new locations, where the environmental variables are known but the species have not been sampled to produce continuous maps of the species' potential distribution. Similarly, the model can be used with maps of future environmental variables to project the shifts in the species' potential distribution caused by climate change (Cheung et al., 2009; Elith et al., 2010; Elith and Leathwick, 2009; Peterson et al., 2015).

In this study, an EHM was used to simulate the abundance of *Ostreopsis cf. ovata* in the Western Mediterranean basin, under current and future climate conditions. *Ostreopsis cf. ovata* abundance time series were obtained as part of long-term monitoring programs. Reanalysis of physical and biogeochemical data of the Mediterranean Sea were statistically corrected to match in situ environmental conditions with the aim of using them as predictors of *O. cf. ovata* cell abundance. Current and future climate simulations were also statistically corrected to fit the distribution of reanalysis. The habitat model, once calibrated and tested, was used to identify the main environmental variables influencing the distribution patterns of *O. cf. ovata* and to shed light on what drives the

occurrence of large blooms in certain regions. Finally, future trends in bloom dynamics were assessed under a high greenhouse gas emission scenario (RCP 8.5).

Numerous experimental studies conducted on *O. cf. ovata* suggest that temperature, phosphate and nitrate concentrations are the most important predictors of its abundance (e.g. Drouet et al., 2022; Jauzein et al., 2018; Ellwood et al., 2020). It is anticipated that higher values of these environmental parameters will correlate with an increase in the abundance of *O. cf. ovata* benthic cells. Additionally, increased hydrodynamics are expected to reduce abundances due to the potential resuspension of benthic cells in the water column (not sampled in the present study).

2. Material and methods

The success of any habitat modeling approach hinges on the availability of (i) a dataset of species abundance/presence that spans a sufficiently wide range of environmental conditions to delineate the habitat (Elith et al., 2010) and (ii) gridded fields of environmental variables of sufficient resolution to capture the conditions in which the observations were made (Adachi et al., 2019). In addition, for climatic projections, it is paramount that (iii) the fields of environmental conditions are consistent between historical (up to current time) and future periods, which means they must come from the same model run, and one the model does not assimilate observed data in the historical period. Otherwise, any change between historical and future distributions would be attributable to a shift in the modeling method rather than to climate change.

The following section outlines efforts to meet three specified conditions. First, the 10-year monitoring programs are introduced, providing data on *O. cf. ovata* abundances. Second, the regional climate and biogeochemical models are presented, simulating the environmental predictors' values. Third, finer scale model products and two sets of in situ data used to refine the regional models and ensure a better match with the statistical distributions of environmental conditions associated with recorded cell abundance. The series of statistical corrections applied notably include a Cumulative Distribution Function transform (CDF-t; Michelangeli et al., 2009, Vrac et al., 2012). Fourth, the implementation of the EHM methodology is presented. The description of all datasets, including details regarding the period retrieved, spatio-temporal resolutions and extent are provided in Supplementary

(Tables A1, A2, A3, A4, A, Fig. A1).

2.1. *Ostreopsis cf. ovata* abundance data

Monitoring and research projects were carried out in France (Villefranche-sur-Mer), Monaco (Larvotto beach), and Spain (Llavaneres) between 2007 and 2017, approximately weekly during June, July and August (and more occasionally beyond this period; Fig. 1 and Table A.1). These months cover the whole blooming period, namely, the detection of the first cells (lag phase or initiation), the exponential increase (exponential phase), the population at blooming abundances (maintenance phase) and the start of the decay of the bloom. This study is built on the benthic, epiphytic *O. cf. ovata* cells, because this form constitutes the bulk of the population and plays a crucial role as a reservoir for blooms (Mangialajo et al., 2017).

At each location, 5 to 15 g of fresh weight (FW) of the most common macrophytes (usually a mixture of *Ellisolandia elongata* (J.Ellis & Solander) K.R. Hind & G.W. Saunders, *Halopteris scoparia* (Linnaeus) Sauvageau, *Jania rubens* (Linnaeus) J.V Lamouroux *Padina pavonica* (Linnaeus) Thivy, and *Dictyota* sp. (Linnaeus) Thivy) were carefully sampled to avoid the detachment of *Ostreopsis* cells (Jauzein et al., 2018). In Villefranche-sur-Mer and Monaco, the sampling methodology followed Drouet et al., 2022. Depth of sampling is around 0.5 m (see Cohu et al., 2013). Macroalgae and the surrounding seawater were transferred in a 250 mL plastic bottle that was closed under water. The whole sample was fixed with acidic lugol and kept at 4 °C, in the dark. In the laboratory, the bottles were shaken to release epiphytic *O. cf. ovata* cells from the macroalgae and the water was filtered through a 500 µm mesh. Macroalgae were transferred back to the bottle, 100 mL of filtered seawater were added, and a new shaking and filtration were conducted. This procedure was repeated a second time. All filtered samples were merged and the total seawater volume was noted. Macroalgae were gently pressed to eliminate excess water and placed onto a tin foil for fresh weight measurement. *Ostreopsis cf. ovata* cells were counted with a 1 mL Sedgewick-Rafter Counting Cell under a light microscope. *Ostreopsis cf. ovata* abundance was expressed as the number of cells per gram of fresh weight of macroalgae (cells.g⁻¹ FW). In Llavaneres, the procedure was slightly different. Macroalgae were transferred to a bottle containing 180 mL of in situ seawater filtered on GF/F and vigorously shaken for 1 min. The water was filtered through a 200 µm mesh and fixed in the same manner as above. The two procedures were compared

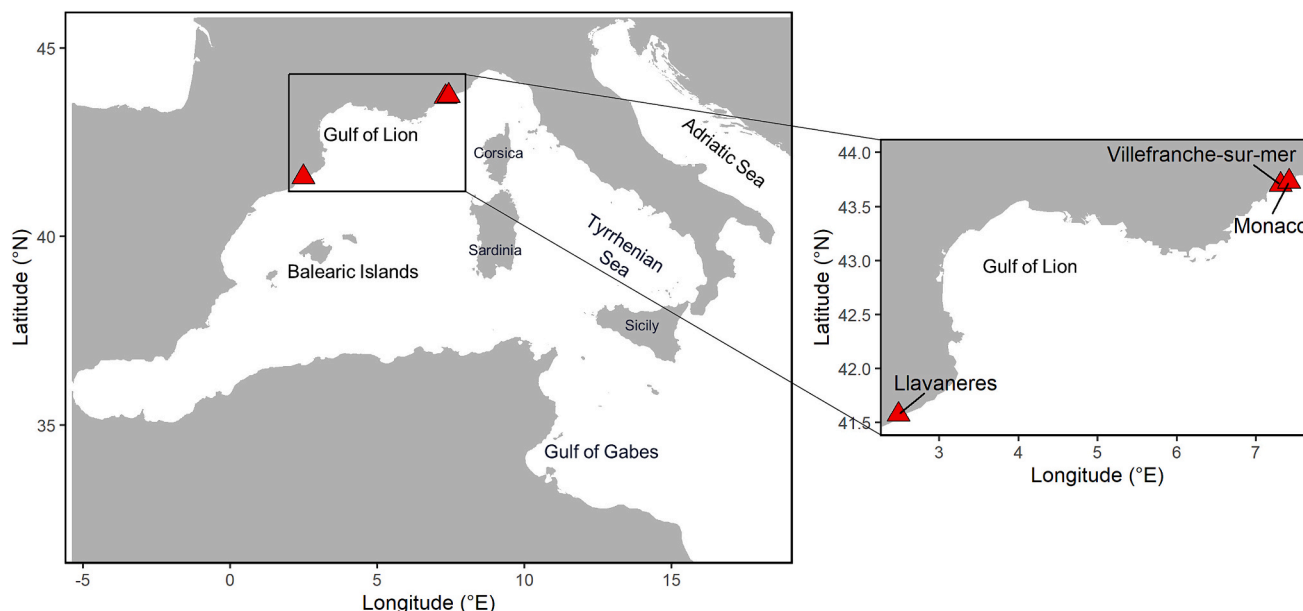


Fig. 1. Location of sampling stations in the North-Western Mediterranean Sea included in this study.

and no significant difference could be detected (Berdalet and Vila, unpublished).

2.2. Environmental predictors

2.2.1. Description of datasets

2.2.1.1. Physical climate model - CNRM-RCSM4. The physical properties of seawater have been simulated by a regional climate model, run as part of the Med-CORDEX initiative (Ruti et al., 2016). Med-CORDEX provides a large ensemble of high-resolution future climate change simulations for the Mediterranean Sea (Darmaraki et al., 2019; Soto-Navarro et al., 2020). However, due to computational and data-availability constraints, only one of the available regional climate simulations was used: the 1950–2100 scenario simulation performed with the CNRM-RCSM4 (Centre National de Recherches Météorologiques - Centre Européen de Recherche et de Formation Avancée en Calcul Scientifique 4) coupled regional climate system model (Sevault et al., 2014), itself driven by the CMIP5 CNRM-CM5 global climate model (Voldoire et al., 2013) following a high greenhouse gas emission scenario (Representative Concentration Pathway 8.5, RCP8.5). The CNRM-RCSM4 model simulates the historical and future evolution of the oceanic, atmospheric, land surface and river components of the Mediterranean climate system and has been widely evaluated and used to study past and future evolutions of the Mediterranean Sea (Darmaraki et al., 2019; Pagès et al., 2020; Sevault et al., 2014). The authors are aware that, by using only one socio-economic scenario and only one physical simulation chain among many other possibilities, the study does not explore the uncertainties associated with any future climate projection. It explores only one of the plausible future, which should be kept in mind when interpreting the results.

Sea temperature, salinity, and the zonal (u) and meridional (v) components of currents were retrieved for the first 6-m thick vertical layer (<https://www.medcordex.eu/>, accessed 2020-03-20). From the North to the South of the domain, the horizontal resolution of the model's ocean grid meshes varied from 9 to 12 km. The daily data over the whole 1950–2100 period was averaged and cut to obtain weekly values for three periods, called historical (1999–2017), mid-century (2041–2060), and end-century (2081–2100). The u and v components of the current were transformed into an along-shore component (current *tr*: toward the right when looking at the coast) and a cross-shore one (current *tc*: toward the coast), assuming those are more relevant to *O. cf. ovata* cells living on the coast. More information about the CNRM-RCSM4 model and its evaluation can be found in Sevault et al. (2014) and about the scenario simulation in Darmaraki et al. (2019).

2.2.1.2. Biogeochemical model - Eco3M-S. The biogeochemical variables (nitrate-NO₃, phosphate-PO₄, dissolved oxygen, and chlorophyll-a concentrations) were simulated by the Eco3M-S model, which represents the dynamics of key elements (carbon, nitrogen, phosphorus, silicon, oxygen) and plankton groups (Ulses et al., 2021). In our context, the Eco3M-S model was forced by the physical CNRM-RCSM4 simulation described above and weekly-averages of the mentioned variables were computed over the same three periods. This Eco3M-S scenario simulation was already used in Moulec et al. (2019) to assess the future evolution of Mediterranean Sea ecosystems.

It is worth noting that climate model scenario simulations aim to produce plausible climate statistics for any period simulated under a given forcing for past or future periods. However, due to the intrinsic chaotic nature of climate (often referred to as the “butterfly effect”), climate scenario simulations do not match the observations at any precise point in time or space. Thus, they can be evaluated or used for their statistical representation of the climate but not for their temporal correlation with the observations. In addition, the spatial grid of the ocean component of CNRM-RCSM4 is relatively coarse (between 9 and 12 km

for North to South of the domain) as is its vertical resolution, therefore not representing well the study area. To approach the real conditions better, reanalysis products from Marine Copernicus Environment Monitoring Services (CMEMS) were used (see Section 2.2.1.2). By combining historical in situ and satellite data with model simulations the so-called data assimilation technique, these reanalysis reconstruct past climate conditions and generate fields of multiple variables that match observations as best as possible (Cossarini et al., 2021).

2.2.1.3. Copernicus reanalysis. The reanalysis distributed by the Copernicus Marine Environment Monitoring Service (CMEMS, MED-SEA_MULTIYEAR_BGC_006_008 <http://marine.copernicus.eu/services-portfolio/access-to-products>, accessed 2020-03-20) was used. All variables were extracted for the surface layer (1.42 m depth) and the 1999–2017 period, over a grid of size 0.0625°. Physical variables (temperature, salinity, u and v components of current) were available at daily temporal resolution and were averaged weekly. Biogeochemical data (nitrate, phosphate, dissolved oxygen, and chlorophyll-a concentrations) were provided as weekly averages (G. Cossarini, pers. comm.).

While those reanalyses are much closer to the reality (by combining past observations with models to generate consistent time series), they still represent average conditions over pixels of size ~6 km × 6 km. Even for pixels along the coast, this still covers mostly offshore waters, while *O. cf. ovata* develops in very shallow coastal waters. To represent these coastal conditions better, two in situ, coastal, measurement data sets were collated (Sections 2.2.1.4 and 2.2.1.5).

2.2.1.4. Coastal data - SOMLIT. In situ measurements of temperature, salinity, and concentrations of nitrate, phosphate, dissolved oxygen, and chlorophyll-a, were gathered from the database of the SOMLIT network (French monitoring network for coastal environments, <https://www.somlit.fr/> accessed 2020-11-08). The bi-monthly measurement were extracted in the surface layer for three stations (Point B: 43°41N, 7°19E, Frioul: 43°15N, 5°18E, and SOLA 42°29N, 03°09E) in the period 1999–2017.

2.2.1.5. Local data. Together with the monitoring of *O. cf. ovata*, described in the previous section, temperature and salinity measurements were taken with a microprocessor conductimeter WTW (Model LF197) on the day and at the site where biological samples were collected, in Monaco and Villefranche-sur-Mer (France). Other environmental parameters were unfortunately not measured during the french survey.

2.2.2. Statistical correction of environmental datasets

To model the abundance of *O. cf. ovata* as accurately as possible, environmental datasets need to match the abundance records: weekly resolution, representative of local (extremely coastal) conditions, in the historical and future periods. To achieve this, the following steps were taken (Fig. 2):

- (1) Shift of the coastal in situ temperature records (Section 2.2.1.4) to match the local ones (Section 2.2.1.5), taken immediately along the beach (Fig. A.1);
- (2) Shift of the reanalysed fields (Section 2.2.1.3) to better match the coastal in situ times series (Section 2.2.1.4, with temperature corrected at step 1) and be more representative of coastal conditions;
- (3) Interpolation and transformation of the historical and future regional physical (Section 2.2.1.1) and biogeochemical (Section 2.2.1.2) model outputs to match the statistical properties of the reanalyses (Section 2.2.1.3, corrected at step 2).

The first issue to overcome was using temperature collected during the monitoring program in Monaco and Villefranche-sur-mer to correct

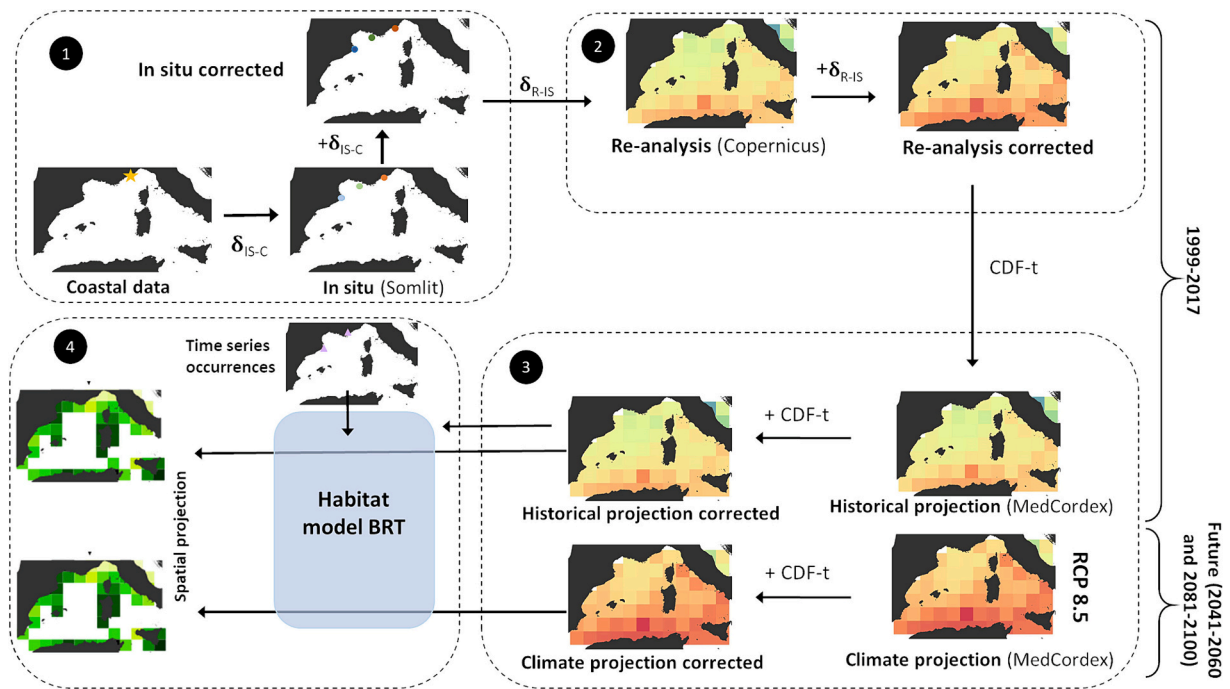


Fig. 2. Flowchart describing the main steps of the methodology used for the present study. Steps are divided in four main parts: (1) Correction of temperature in-situ data δ_{IS-C} (Somlit) from temperature sampled by monitoring programs using a linear regression, (2) Correction of Copernicus data from corrected in situ data with CDF-t approach (CDF-t₁), (3) CDF-t method used to get corrected historical and climate simulations (CDF-t₂), (4) calibration of ecological habitat model and projection across space and time (current, mid- and end-century periods).

the temperature of the “Point B” time series retrieved from the Somlit database. The correction was made by performing a regression, between Coastal and Somlit data (Point B) and corresponds to δ_{IS-C} (Fig. 2 (1)). The regression has a high R-squared of 0.99 (with p -value < 0.001).

Physical (CNRM-RCSM4) and biogeochemical (Eco3M-S) models available, described above (“Description of datasets” section), do not have a sufficient spatial resolution to be directly implemented to an EHM as forcings variables. These models are indeed not able to perfectly reproduce the local climate statistics. Errors or biases can be linked to the model spatial resolution, the misrepresentation of physical processes or external forcings, or simply to the climate chaotic nature. This statement is particularly prevalent in coastal areas where models struggle to describe different processes (Bensoussan et al., 2013). To fill this gap, the CDF-t approach between first used observed coastal data (monitoring program and Somlit database) was applied to correct Copernicus reanalysis (CDF-t₁; Table A.6). This method was then applied between CNRM-RCSM4/Eco3M-S and corrected Copernicus reanalysis (CDF-t₂) to obtain the best product for historical and future environmental data (Figs. 2, A.2). For clarity, the explanation of the CDF-t is based on the application between Copernicus reanalysis and CNRM-RCSM4/Eco3M-S simulations (CDF-t₂). The CDF-t approach has been developed by Michelangeli et al. (2009) to correct biases that can occur in physical and biogeochemical models. CDF-t generally behaves in a much better way than quantile mapping does (Michelangeli et al., 2009; Vrac et al., 2012). A mathematical transformation is applied to the CNRM-RCSM4/Eco3M-S CDFs to define new CDFs as close as possible to the CDFs of corrected reanalysis. The CDF-t’s strength is to consider the CDF change between historical and future CNRM-RCSM4/Eco3M-S simulations. CDF-t mathematical transformation was calibrated between CNRM-RCSM4/Eco3M-S and corrected reanalysis for each environmental variable available and applied separately. All coastal available pixels were used (see Fig. 4b) with a weekly time resolution for each dataset. New CDFs were then applied to the CDFs of CNRM-RCSM4/Eco3M-S for current, mid-century and end-century periods at the same spatial and temporal resolution.

In the present study, all computations related to the statistical adaptation have been made through the CDF-t R package (Vrac and Michelangeli, 2015). More theoretical and technical details can be found in Michelangeli et al. (2009).

In addition, as the spatial resolution was different between Copernicus and CNRM-RCSM4/Eco3M-S datasets, the later were interpolated to the resolution of Copernicus data ($0.0625^\circ \times 0.0625^\circ$) using nearest-neighbor approach and “FNN” R package (Beygelzimer et al., 2024).

The slope of change was derived for each predictors by fitting a linear model between the point of focus and four points before it. The slope was computed to capture the dynamic of changes in the environmental predictors. U and v , representing the zonal (east-west) and meridional (North-South) components of the current, respectively, were transformed into three different current components: current along shore (component of the ocean current that flows parallel to the coastline), current cross shore (current flowing across the shore, perpendicular to the shoreline), and total current speed. To calculate these variables, the azimuth relative to the coast was computed for each pixel in the projected areas. The azimuth represents the angle between the shore and a reference direction (the North), providing the orientation of the shore for each pixel. Once the azimuth was determined, the equations below allowed to derive new environmental variables:

$$\text{current along shore} = u \cdot \cos(\text{azimuth}) - v \cdot \sin(\text{azimuth})$$

$$\text{current cross shore} = u \cdot \sin(\text{azimuth}) + v \cdot \cos(\text{azimuth})$$

These two equations transform the zonal (u) and meridional (v) components of the flow into the components of the current along the azimuth angle and perpendicular to it.

$$\text{current speed} = \sqrt{u^2 + v^2}$$

This equation uses the Pythagorean theorem to compute the intensity of the current.

2.3. Ecological habitat model

Extreme gradient boosting (XGBoost) modeling approach (Chen and Guestrin, 2016) was used to model *O. cf. ovata* abundances. XGBoost is an efficient gradient machine learning method, which combines two algorithms: 1) simple and small regression trees, calculated on random subsets data while minimising residuals and, 2) subsequently, boosting which combines all the models in a unique solution. XGBoost models can fit complex functions, which could reflect the complexity of *O. cf. ovata* processes patterns.

Prior to modeling, environmental data were extracted by matching the date and localities of the biological sampling points with the closest pixels and date of Copernicus reanalysis corrected (environmental characteristics at each sampling point are provided in Fig. A3). The collinearity between predictors was then tested to limit possible biases in predictors contributions, model predictive performances and presence of spatial autocorrelation (Dormann et al., 2013). Variance inflation factors and a Spearman pair-wise correlation test between predictors were performed. One of the two descriptors was removed when correlation values of r_s were above 0.8 (Dormann et al., 2013). These analyses were performed using the `usdm` and `corrplot` R package (Naimi et al., 2014; Wei and Simko, 2021). The selected environmental predictors are: temperature, salinity, phosphate concentration, nitrate concentration, chlorophyll-*a* concentration, current along shore component, current cross shore component, current speed and dissolved oxygen concentration with all slope values associated. Range values across *Ostreopsis* sampling points are in Table A.7.

XGboost parameters (number of trees, learning rate, minimum sum of weights of all observations required in a child and maximum depth) were determined by using 4-fold cross-validation and gaussian distribution. Different distributions (tweedie, poisson, quantile) were tested but with inconclusive results or bad predictive performance. Before calibration, abundance data were \log_{10} transformed to get closer to a Gaussian distribution. Best parameters were selected by minimising the root mean square error (RMSE) on the validation portions, to avoid possible overfitting (provided in Fig. A.4). The selected parameters are number of trees = 600, minimum sum of weights of all observations required in a child = 6 and maximum depth = 4, and learning rate = 0.01. The final XGboost model was used to predict *O. cf. ovata* abundances. Two R^2 were produced: a predictive R^2 obtained during the cross-validation approach and a descriptive R^2 obtained with the full model using all the predictive and observed abundance values.

The relative contribution of the environmental predictors to the model was calculated by the gain (mean \pm SD) which takes each predictor's contribution for each tree in the model. A higher value of this metric when compared to another variable implies that it is more important for generating a prediction. The variable importance scores were scaled between 0 (least important) and 1 (most important).

Partial dependence plots (pdp) were computed to examine the univariate marginal effect of the most important predictors according to the dependent variable in 100 resamples (Friedman, 2001). Specific values (in the predictor range) were assigned to the variable of interest in the training set while the others remained at their original values. Average prediction was performed for each resample and a mean and standard deviation were calculated for the 100 resamples. This approach was implemented for the full range of each predictor at each decile. Pdp were performed using R package 'pdp' (Greenwell, 2017).

Finally, fitted models were finally projected according to the historical period (1999–2017) and future scenarios (mid-century: 2041–2060; end-century: 2081–2100). The projected area focused on the western part of the Mediterranean Sea (5.5°W, 19°E, 32.5°N, 46°N).

To define the projected area of EHMs, the authors used literature and expert knowledge on *O. cf. ovata* biology, ecology and bloom dynamics. The microalgae grows in shallow coastal ecosystems and is described as mainly epiphytic of macroalgae and phanerogam meadows but also proliferates attached to hard-rock and sand substrates (Cohu et al., 2013;

Gémin et al., 2020). Maps of habitat types from EMODnet (<https://www.emodnet-seabedhabitats.eu>, accessed 2020/03/20) was used and retained pixels covered by at least 5 % of the following habitat types: rock or other hard substrates, mixed sediment, coarse sediment, coarse and mixed sediment, dead and alive meadows of *Posidonia oceanica* and *Cymodocea nodosa*. Mud and sand habitats were not considered as *O. cf. ovata* is not typically found in these substrates. Only the pixels closest to the shore line were retained. The projected area is in Fig. 4b.

From these, spatial mean abundances per pixel across time for each period were computed. The seasonal dynamics statistics (median, quantiles 5 %, 25 %, 75 % and 95 %) on each period at the scale of the Mediterranean Sea were extracted. To assess the persistence of the bloom, the mean number of weeks when abundances above given a threshold for each period was also computed. The selected threshold is the quantile 90 of abundances in the current period.

3. Results

This section presents the results of the ecological habitat model performance and the shape of the relationship between abundance and abiotic predictors through the analysis of the partial dependence plot. The assessment of the spatio-temporal abundance dynamics across space and time for the current period, mid- and end-century is then described.

3.1. *Ostreopsis cf. ovata* ecological habitat model performance

Different performance metrics scores were produced using 4-fold cross-validation and the full model to evaluate the performance of the models. The first metrics provides the descriptive power of the model based on the model fitted on all observations (no cross-validation). In the space where the model is fitted (\log_{1p} -transformed) the descriptive R^2 is equal to 0.9 whereas in the original scale the associated R^2 falls to 0.33. The model was initially fitted on bootstraps of the data (to tune the parameters). For each bootstrap, some observations were not selected, which allow estimating the quality of the predictions. According to prediction obtained from the cross-validation procedure, predictive R^2 has a value of 0.46 in \log_{1p} -transformed and 0.009 in the original scale. These results highlight a biased estimation of the prediction where low abundances tend to be overestimated, while high abundances seem to be underestimated (Fig. A.5).

3.2. Current trend

The partial dependence plot (pdp) gives some insights into how a species might respond to a given environmental variable. Pdp's are shown in Figs. 3 and A.6, ordered according to the environmental predictors' importance to EHMs (only the first six more important variables are displayed). The feature importance measured by the gain (\pm SD) indicates which best capture abundance patterns and explain the current species habitat.

The most important predictors of *O. cf. ovata* bloom intensity, determined by the maximum cell concentrations attained, are seawater temperature, seawater temperature slope and chlorophyll *a* slope (Fig. 3), with a score ca. 0.26 (\pm 0.069), 0.15 (\pm 0.08) and 0.072 (\pm 0.02), respectively. They are followed by salinity, phosphate (PO₄) and nitrate (NO₃) concentrations with score values of 0.05 (\pm 0.01), 0.48 (\pm 0.01) and 0.46 (\pm 0.01) respectively (Fig. 3). Expected abundances increase with increasing values of these predictors with particularities. Namely, temperatures from 24 to 26 °C constitute an upper optimal limit for bloom intensity. High abundances are also found for high salinities values whereas salinities below 37.5 were not recorded in the three sites.

For the chlorophyll-*a* slope, the ideal situation seems to be when chlorophyll-*a* increases slightly (i.e. slope a bit above 0) corresponding to the end of the blooming period; in contrast, decreases (after the bloom) or strong increases (bloom initiation) are less favourable. Similarly, the predicted abundance relative to the slope of temperature is

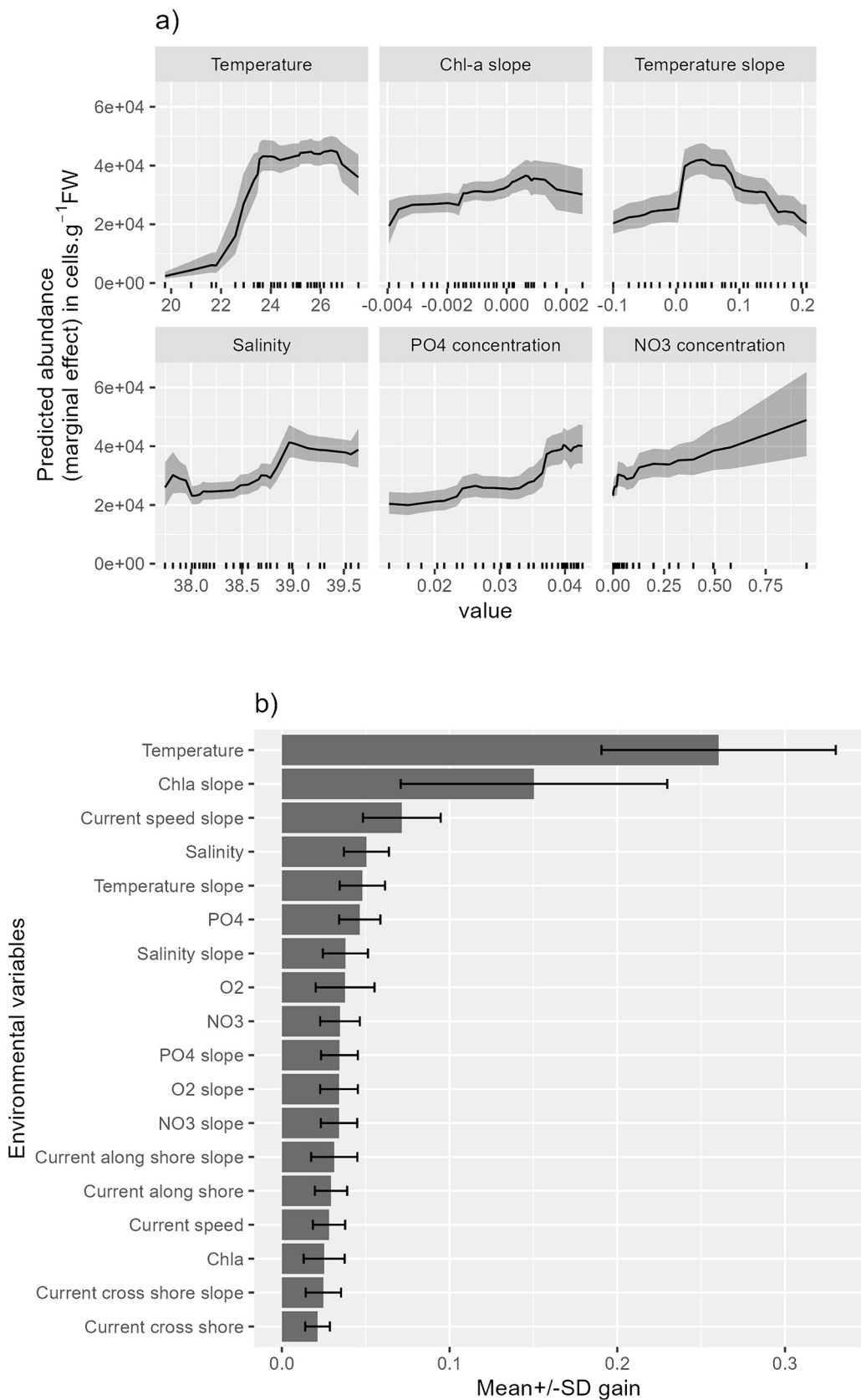


Fig. 3. a) Partial dependence plots showing the influence on mean *O. cf. ovata* cell abundance by the six most important environmental predictors in our XGBoost model, ordered by their relative influence, b) distribution of the order of importance of variables in the model.

maximal when that slope is increasing rather slowly. Temperature increases (corresponding to the beginning of spring/summer) and decreases (end of summer) do not correspond to good conditions. NO₃ and PO₄ concentrations appear to have a positive relationship with cell abundance, while the remaining 12 variables (Fig. 3b, salinity slope, cross-shore current, chlorophyll-a, etc.) would play a less important role

in the model.

Monitoring samples tend to reveal a bloom beginning in June and lasting until October. These observed abundances range from 1·10¹ cells·g⁻¹ FW of macroalgae to 1·10⁶ cells·g⁻¹ FW of macroalgae, with a maximum of ~8·10⁶ cells·g⁻¹ FW of macroalgae in Llavanes (Fig. 4a). The bimodal distribution of observations is certainly due to the high

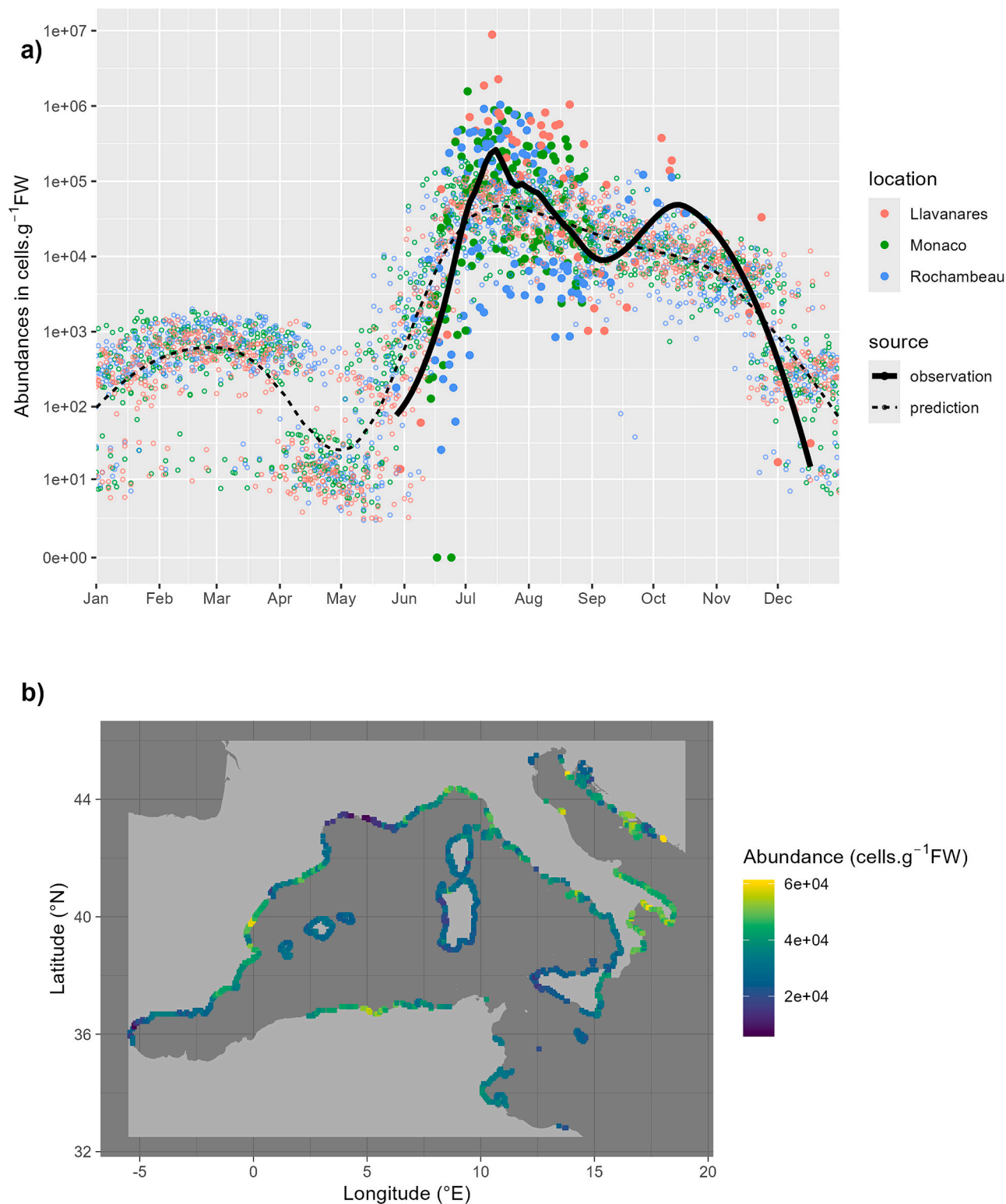


Fig. 4. a) Seasonal variability of the *Ostreopsis cf. ovata* cell abundances in the sampling localities (France, Spain and Monaco) in the present period (solid line/point) and model prediction (dash line, transparent dot) in the present period (1999–2017), y-axis is in log scale. A loess regression for each category was applied with a span of 0.15, b) modelled summer (June, July, August) mean abundance of *Ostreopsis cf. ovata* cells·g⁻¹ FW in the Western Mediterranean Sea in the current period.

heterogeneity of sampling effort, with more samples in summer and fewer in autumn. The pattern of EHM projected on corrected climate models follows a similar trend as he observed data, with less intensity during the summer when the blooms traditionally occur. Models were also projected for periods not sampled during the monitoring program (winter/spring) where abundances vary between $1 \cdot 10^2$ and $1 \cdot 10^3$ cells·g⁻¹ FW macroalgae but never reached zero.

In summer, the highest modelled current abundances are situated along the Catalan and Valencian coasts in Spain, in South-Eastern France, Southern Italy, the Adriatic Sea, and Algeria with $>4.5 \cdot 10^4$ cells·g⁻¹ FW (Fig. 4b). In contrast, the lowest modelled abundances ($<1 \cdot 10^4$ cells·g⁻¹ FW) are mainly found in the Gulf of Lion. Intermediate values (between $1 \cdot 10^4$ and $4.5 \cdot 10^4$ cells·g⁻¹ FW) would be found in many coastal areas such as Eastern Italy or other parts of the French and Spanish coasts.

The spatio-temporal dynamics provided by the model of *O. cf. ovata* blooms are represented by the number of weeks when abundances exceed the 90th percentile (Fig. 5). Blooms seem to begin in June in the Gulf of Gabes, Southern Italy, and last mainly for one to two weeks in the month. July is the most intense period, with blooms persisting throughout the month in Southern Italy, the Adriatic Sea, and a few localities in South-Eastern France. Along the Spanish coast, in North Africa, Eastern Adriatic Sea, and the North of Corsica and Sardinia, *O. cf. ovata* could persist for two to four weeks. In the other regions, the blooming period is usually one week (Southern Sardinia, Gulf of Gabes, Gulf of Lion, Balearic Island). The bloom lasts two to three weeks in August along the Spanish coasts and in North Africa, with a patchy distribution along the Italian coasts.

3.3. Effect of climate change on the seasonal of *O. cf. ovata* dynamics and prediction on their summer spatial distribution

The seasonal dynamics across the whole study area were extracted and plotted according to the time for the three periods, the current period (1999–2017), the mid-century period (2041–2060), and the end-century period (2081–2100) in Fig. 6.

Under the current period (1999–2017), the model shows the lowest abundances occurring during winter and spring (January to May), the same pattern as observed in the monitored localities (Fig. 4a). Increase in abundance starts in June and reaches maximum abundances (median $\sim 3.8 \cdot 10^4$ cells·g⁻¹ FW macroalgae) in July. The 5 % and 95 % prediction vary between $1 \cdot 10^3$ and $\sim 1 \cdot 10^6$ cells·g⁻¹ FW macroalgae in summer, consistent with the spatio-temporal heterogeneity of the species (Fig. 5). A slow decline in abundance occurs at the end of the summer until November.

Concerning the simulated future evolution of the *O. cf. ovata* abundance under the RCP8.5 scenarios, two patterns are discernible (Fig. 6). Firstly, the magnitude of the bloom intensity, in terms of cell concentrations during the summer/fall period is similar to the current period. Secondly, the bloom's time window will progressively extend, starting earlier in the year -before June for the mid-century and mid-May for the end-century- and lasting until mid-November for the mid-century and December for the end-century (Fig. 6).

Summer mean abundances in future scenarios were compared to the historical period (indicate years) by computing their differences (Fig. 7). The projections reported high spatial variations. By the mid-century (2041–2060; Fig. 7a), averaged abundance could increase slightly along the Spanish coasts, Northern Africa and in the Balearic Islands, and could decrease although very weakly in Eastern France and Southern Italy. By the end-century (2081–2100; Fig. 7b), while

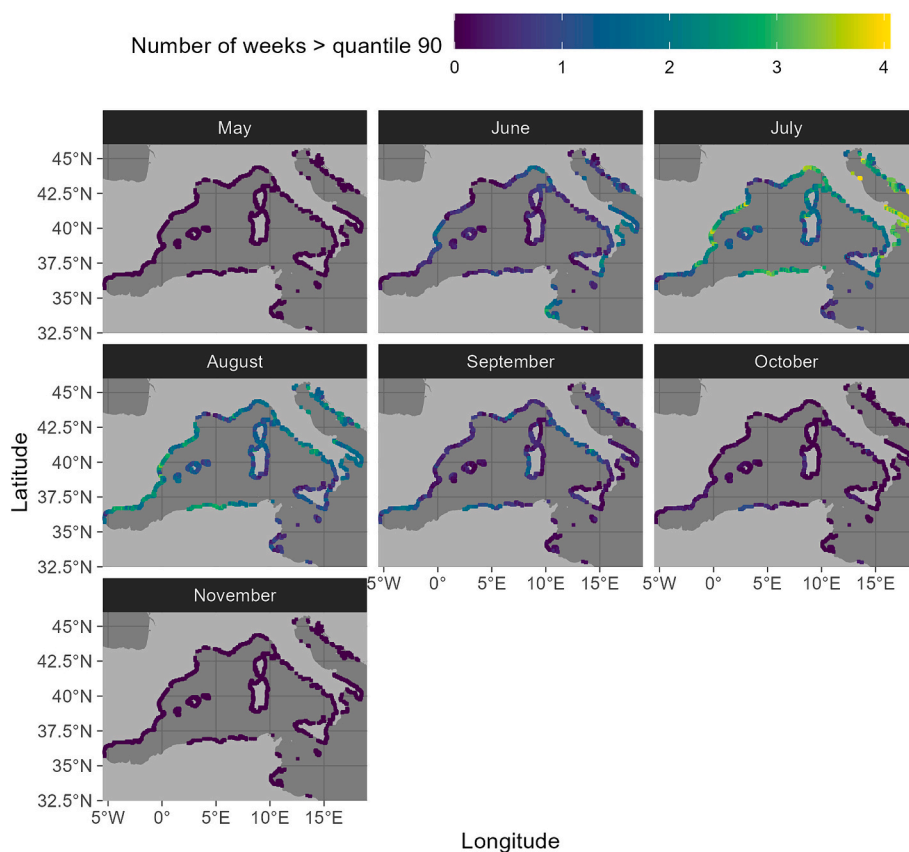


Fig. 5. Spatio-temporal dynamics between May and November of the bloom expressed in the mean number of weeks above quantile 90 of abundances (here above $4.2 \cdot 10^4$ cells·g⁻¹ FW).

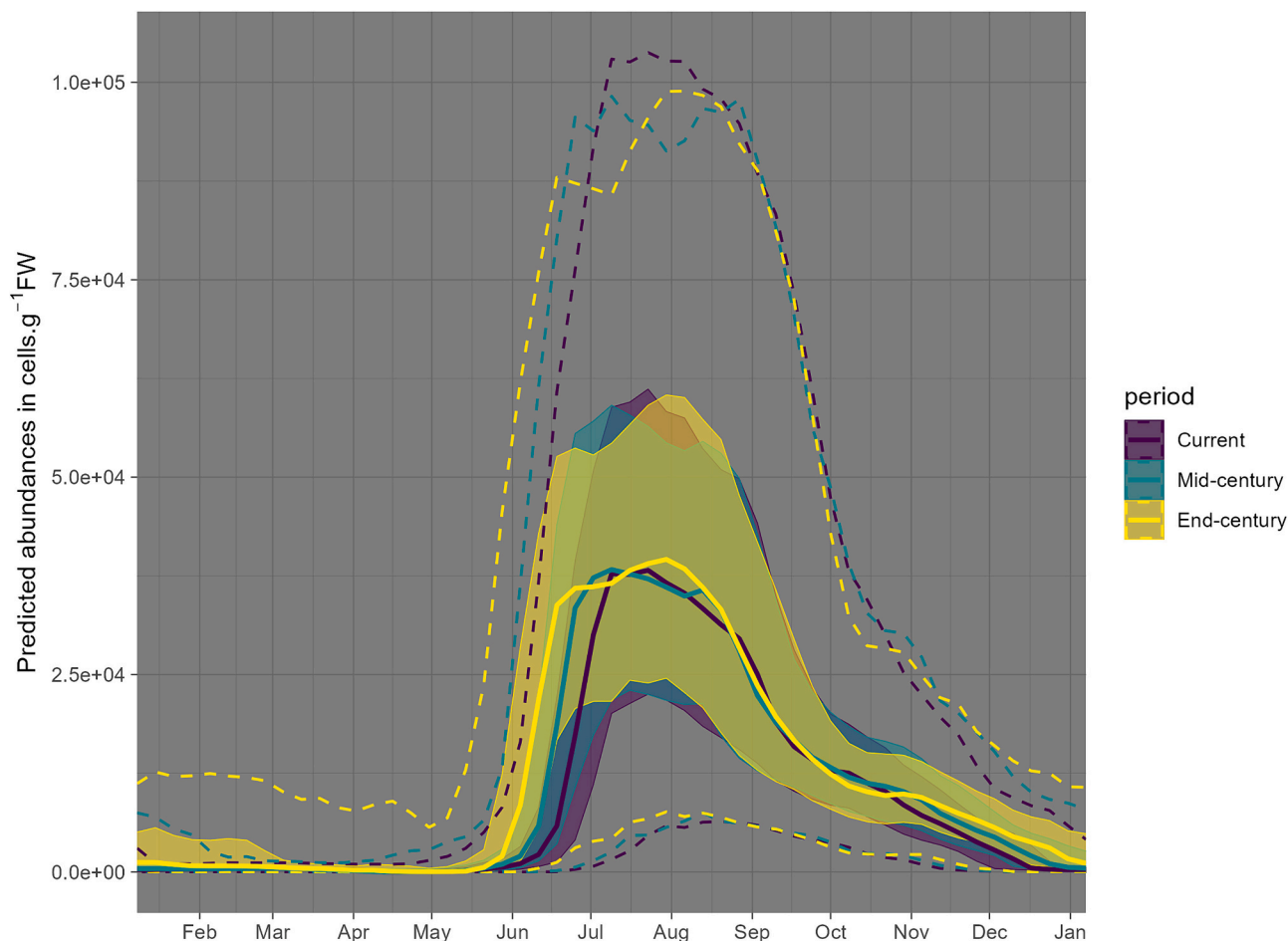


Fig. 6. Seasonal distribution of the abundances of *Ostreopsis cf. ovata* in the Western Mediterranean basin in the present, mid-century and end-century periods. Solid line represents weekly median values with shaded areas indicating quantiles 25 and 75 and dashed lines indicating quantiles 5 and 95 computed at the scale of the study area.

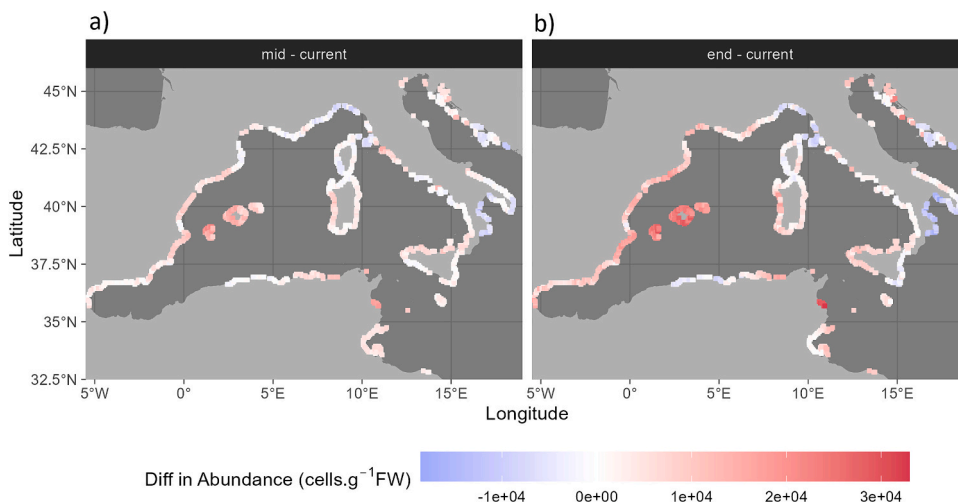


Fig. 7. Difference between the mean summer abundances of *Ostreopsis cf. ovata* projected based on RCP8.5 scenario with respect to present values for a) the mid-century and for b) the end-century. Negative values (blue) are related to a decrease in mean summer abundance whereas positive values (red) to an increase.

abundances would still decrease in these areas, high increases are simulated along Spanish and French coasts and in the Balearic Islands, Adriatic Sea and North Africa.

The changes in the spatio-temporal bloom dynamics are heterogeneous across the Western Mediterranean Sea (Fig. 8). Spanish and

Balearic coasts are characterized by an increase in the number of weeks above the selected threshold (here, quantile 90) of around one week in the mid-century and between two to three weeks in the end-century for the summer period (June, July, and August), when less than four weeks per month achieved this threshold. The Italian coasts show a moving

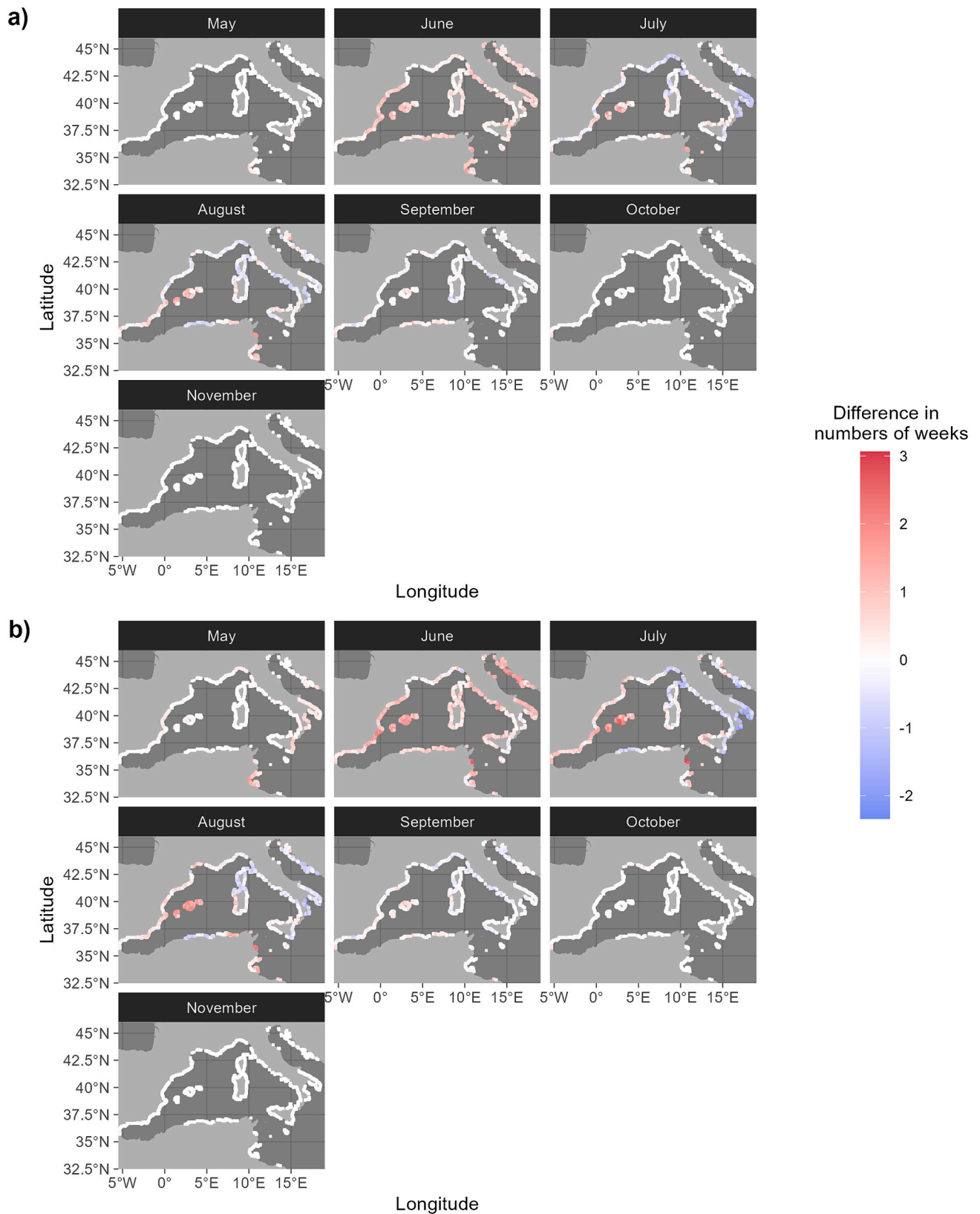


Fig. 8. Changes in the spatio-temporal *Ostreopsis cf. ovata* bloom dynamics between May and November), expressed as the difference in the mean number of weeks above quantile 90 of abundances (here above $4.2 \cdot 10^4$ cells \cdot g⁻¹ FW) for a) the mid-century (2041–2060) and for b) the end-century (2081–2100) with respect to the present climate.

temporal window with an increase in the number of weeks in June (one or two weeks) and a decrease in July and August. In North Africa, bloom occurrences should expand in June and persist in the Gulf of Gabes until August, while a decrease is observed along Algerian coasts in August.

4. Discussion

The present study developed a framework for using an innovative statistical adaptation chain combining a global climate model, regional climate models, statistical downscaling and EHMs to improve the prediction of how global climate change may affect the spatial pattern and temporal dynamics of *O. cf. ovata* blooms in the Western Mediterranean Sea.

4.1. Predictive performance of EHMs to model *Ostreopsis cf. ovata* abundance

The cross-validation procedure produced an unexpectedly low R^2 while limiting the model overfit by minimising the RMSE (Fig. A.4). R^2 score obtained between observed and predicted data from the full model was high but the model under-predicts high abundances and over-predicts low abundances (Fig. A.5). R^2 is known to be sensitive to the extent of dependent variables (Gelman and Hill, 2006) which range between $17.5 \text{ cells}\cdot\text{g}^{-1}$ FW macroalgae and $8\cdot 10^6 \text{ cells}\cdot\text{g}^{-1}$ FW macroalgae in this study. This could explain the low cross-validated R^2 which is compounded by the small amount of data available. This bias is reflected in the projection across space and time with for example summer mean abundances which do not exceed $6.2\cdot 10^4 \text{ cells}\cdot\text{g}^{-1}$ FW macroalgae (Fig. 4b).

Most EHMs studies mainly use presence/absence or presence-only data as dependent variables (Benedetti et al., 2018; Fabri-Ruiz et al., 2019; Gomes et al., 2018; Liu et al., 2016; Phillips et al., 2009). In the present study, species habitat was modelled using cells abundance data. It is known to provide greater ability to delineate species' range boundaries and produce more accurate models (Howard et al., 2014; Yates et al., 2018). When presence-absence or presence-only data are used, habitat suitability is partly lost because all presences are treated equally. With abundances, the discrimination of suitable habitat is higher, which is beneficial when EHMs are used to project species distribution across space and time.

4.2. Current temporal dynamics and spatial patterns

This is the first study conducted in the Western Mediterranean basin, that models the large scale patterns and the role of physical and biogeochemical environment on *O. cf. ovata* abundances based on the most recent blooms in the area. The results obtained from current projections indicate high spatial heterogeneity at the scale of the NW Mediterranean Sea. A recent study, aimed to determine the link between *O. cf. ovata* abundances and impacts on human health, identified that symptoms could start during the pre-bloom phase at $2\cdot 10^4$ to $2\cdot 10^5 \text{ cells}\cdot\text{g}^{-1}$ FW, and continue during bloom conditions, with higher abundances of the microalga, namely $2\cdot 10^5$ – $2\cdot 10^6 \text{ cells}\cdot\text{g}^{-1}$ FW (Berdalet et al., 2022). In this study, the obtained values are clearly below these thresholds. This can be related to the difficulty of capturing extreme values in the models.

In the model, high mean abundances and blooms observed in summer along the Catalan coast (Fig. 4a, b) are consistent with the main reports on proliferation which occurred in this region and were related to some mild cases of respiratory irritations and general malaise (Vila et al., 2016, 2012, 2008). Along the Tyrrhenian coasts, similar symptoms have been documented in parallel with high cell abundances in beaches affected by recurrent summer blooms (Ciminiello et al., 2014, 2013; Penna et al., 2005; Zingone et al., 2006). Some regions such as Taormina in Sicily (Italy) are known for recurrent *Ostreopsis* spp. toxic blooms every summer (Ciminiello et al., 2013).

In the model, high abundances and bloom extension in July/August are observed in the Adriatic Sea. This is contrary to previous findings indicating that blooms traditionally occur in early fall (end of September) (Mangialajo et al., 2011). It is known that different population of *O. cf. ovata* exists in the Mediterranean Sea. A DNA fingerprinting technique provided emerging evidence about the presence of two distinct populations in the Eastern and Western basins (Italiano et al., 2014) by toxicological profile (Guerrini et al., 2010) and ecological data (Mangialajo et al., 2011; Totti et al., 2010). Populations from different coastal areas should display marked differences in the bloom time. However, in the present study, EHMs were performed with data from the French, Monegasque and Spanish coasts but not from the Adriatic Sea which could explain the differences. The amount of biological data was however not sufficient to test this hypothesis.

Bloom occurrences along French and Monegasque coasts were expected as high abundance of epiphytic because cells were already detected (Cohu et al., 2013, 2011).

In the model, *O. cf. ovata* dynamics followed a marked seasonal variability as previously described in different regions of the NW Mediterranean basin (Accoroni et al., 2015; Cohu et al., 2013; Mangialajo et al., 2011; Vila et al., 2016). However, the literature and observed data depict the existence of two peaks in summer (July–August) and autumn (September–October) that the model does not capture (Fig. 4a; Mangialajo et al., 2011, Scalco et al., 2012). Considering monitoring programs occur mostly in summer as the bathing season generally ends in September, there is insufficient data to adequately feed the model and capture the full scope of seasonal environmental variability. This highlights the necessity for additional research throughout the whole year (including winter time to examine in detail the dynamics of *O. cf. ovata* (including cysts) and more accurately define the species' habitat).

4.3. Relationship between abundance and predictors

Partial dependence plots and variable importance are consistent with *O. cf. ovata* ecology (Fig. 3). The positive relationship between temperature and abundance is consistent with several previous studies (Asnaghi et al., 2017; Carnicer et al., 2015; Cohu et al., 2013; Scalco et al., 2012), although there is no universal role (see revisions by Totti et al., 2010, Tester et al., 2020). A study on the life cycle of *O. cf. ovata* highlighted that temperature is a key factor for bloom onset because it facilitates cyst germination (Accoroni et al., 2014). Regarding in vitro experiments, temperature is recognized influencing on growth rate. Scalco et al. (2012) identified an optimum between 22°C and 26°C and Carnicer et al. (2015) between 24°C and 28°C . The observed optimum temperature window is a bit different, which could be related to the strains origin (Monaco - Larvotto beach, Villefranche-sur-Mer and Llanvaneres). This work shows an optimum temperature range between 23°C and 26°C ; above this threshold temperature seems to limit the growth rate as also documented by Drouet et al. (2022) on the Monaco-French coast. The slope of chlorophyll and temperature is mostly a marker of bloom phenology to capture seasonal dynamics. Nutrient concentrations were also positively associated with *O. cf. ovata* abundance. Nutrients availability is often considered as an important factor in the control of (toxic or not) high biomass blooms. Nutrients are key in determining the initiation and maintenance of the bloom, as well as their decay. Nutrient enrichment of coastal areas is often considered as an explanatory factor. In the case of *O. cf. ovata* in the Mediterranean, some blooms were documented on high nutrient conditions (Accoroni et al., 2011; Meroni et al., 2018). However, no direct link between *Ostreopsis* spp. distribution and phosphate concentration were found in some other areas (Cohu et al., 2011; Vila et al., 2001). Nonetheless, increase in nutrient availability might have an indirect impact on *Ostreopsis cf. ovata* development by fostering macroalgae growth or abundances (Medina-Pérez et al., 2023).

Salinity seems to play a limiting role, as *Ostreopsis* species seem to avoid salinities below 20 and blooms occur at a salinity higher than 37

(Pezzolesi et al., 2012; Pistocchi et al., 2011). In this study, the salinity range is small and above 37 because as monitoring was performed in during summer in stations not affected by permanent and high fresh-water runoff from big rivers that could lead to important salinity fluctuations.

At the scale of the study area, hydrodynamics described by current components depicts low relationship with *O. cf. ovata* distribution. Several studies have highlighted that hydrodynamics could be one of the main factors affecting blooms with higher abundances found in sheltered sites, compared to exposed ones (Chang et al., 2000; Mabrouk et al., 2011; Selina et al., 2014; Shears and Ross, 2009; Totti et al., 2010). However, the results cannot be compared due to the differences in time scales. Blooms occur in very shallow waters and large variations in turbulence over the course of the day appear to imply that cells are released from the macroalgae and transported, whereas in the present study the time resolution is on the order of a week. Further investigations are needed to better characterize “hydrodynamism” at the scale of the *Ostreopsis* blooms to be implemented in EHM.

4.4. Temporal and spatial dynamics according to climate change

Climate change could modify the species growth rate and phenology (Drouet et al., 2021; Figs. 4b and 5). The study's results suggest that the timing of seasonal *Ostreopsis cf. ovata* blooms could start earlier and last longer in the year in the mid- and end-century in an RCP8.5 scenario. The bloom window extension could be related to suitable conditions in spring and autumn, in particular optimal temperature (between 23 °C and 26 °C) and increased salinity (Fig. A.2c).

On the temporal scale, bloom intensity seems to remain at the same range values in future conditions (Fig. 6). However, Figs. 7 and 8 highlight a high spatial heterogeneity in the intensity and duration of bloom occurrences in the Western Mediterranean Sea. The observed increases in abundance in some regions are in line with the established understanding that warmer temperatures can enhance the growth rates of this species (Carnicer et al., 2016; Granéli et al., 2011; Scalco et al., 2012). The suitable conditions have however only occurred in June, and are not persisting in July and August in some areas as observed in Italy and along the Algerian coasts and are indicative of the complex interactions between abiotic and biotic (including cells physiology) factors determining blooms in nature. These results suggest that a high intensity (i.e. with high cell abundances) bloom could persist with the same magnitude or higher, compared to the historical period. These patterns could have important consequences on coastal marine ecosystems, human health, and the economy (see below).

For computational and data availability reasons, the current study only explores one of the possible future evolutions of the Mediterranean Sea under climate change although a major uncertainty affects regional climate change projections (Darmaraki et al., 2019; Soto-Navarro et al., 2020). Therefore, this study mostly focuses on exposing one plausible future trajectory under a strong greenhouse gas emission scenario and developing a methodological approach. It did not intend to identify the most probable changes. In particular, among the existing Med-CORDEX simulations for RCP8.5, CNRM-RCSM4 is one of the least warming models (Darmaraki et al., 2019), which opens the avenue for plausible changes with stronger ecosystem modifications. On the contrary, the RCP8.5 scenario is (unfortunately) a plausible scenario that does not take into account international mitigation strategies to limit greenhouse gas emissions. Therefore, it represents a more pessimistic future than other existing scenarios. Exploring all the sources of uncertainty in future projections of *Ostreopsis cf. ovata* is beyond the scope of this study and probably not feasible today for computational reasons.

4.5. Ecological and economic consequences of current and future *Ostreopsis cf. ovata* patterns

4.5.1. Ecological consequences

In the future, increased abundance and duration of *Ostreopsis cf. ovata* blooms, such as those observed in this study, could increase the exposure of marine organisms to the toxins produced by this dinoflagellate, with unknown consequences for ecosystem functioning. Massive proliferations of *O. cf. ovata* in the Mediterranean Sea are known to have a negative effect at different trophic levels (see Pavaux et al., 2020 for review). Toxins produced by this dinoflagellate have been recorded in many marine organisms such as sea urchins, crabs, herbivorous fish, mussels (Amzil et al., 2012; Biré et al., 2015, 2013). Because benthic cells can be detached from the substrate by hydrodynamics, planktonic or nekton organisms and filter feeders could also be impacted (Biré et al., 2015; Neves et al., 2018; Vila et al., 2016). Mass mortalities of invertebrates, such as sea urchin, related to *O. cf. ovata* blooms, have already been described (Pavaux et al., 2019; Privitera et al., 2012) and reprotoxic effects (impacts on reproduction) have been quantified on copepods nauplii (Guidi-Guilvard et al., 2012; Pavaux et al., 2019).

4.5.2. Human health and economic consequences

If harmful *O. cf. ovata* blooms increase in intensity and duration in some regions of the Mediterranean Sea, the incidence of human syndromes associated with exposure to *Ostreopsis*-produced toxins could increase. Scarce, but dramatic human poisonings due to ingestion of sea products potentially contaminated with toxins of *Ostreopsis* spp. have been documented in tropical regions following consumption of fish or crustaceans (Onuma et al., 1999; Pavaux et al., 2020). In the Mediterranean Sea, toxins produced by *Ostreopsis cf. ovata* can be found in marine organisms and have already reached the threshold set by the European Food Safety Authority (Biré et al., 2015, 2013; Brissard et al., 2014). Fortunately, no seafood poisoning due to *Ostreopsis* toxins has been reported in the Mediterranean zone until now. Most of the time, mass human intoxications due to *O. cf. ovata* blooms in the Mediterranean Sea were related to recreational activities with direct skin and mucosae contact and/or inhalation of seawater aerosols by inhabitants or people conducting professional activities near the sea, including conducting *Ostreopsis* monitoring (Berdalet et al., 2022; Ciminiello et al., 2014; Vila et al., 2016). Often these poisonings are not very dangerous, but they can easily overwhelm hospital emergency facilities, potentially delaying the treatment of other patients.

As previously mentioned, the Mediterranean countries' economy is strongly linked to the sea, through fishing, aquaculture and, above all, recreational beach tourism. Indirect and long-term effects of chronic exposure to HABs caused by *O. cf. ovata* in current and future climate conditions could induce a significant reduction in tourist flow, lost revenue for businesses which serve the hotel or restaurant industry, and a decrease in recreational uses of the sea (Berdalet et al., 2022).

4.6. A new framework for modeling HABs in a context of climate change

EHMs have proved to be a useful, valuable, and cost-effective tool to quantify potential changes in species distribution, especially in data-poor areas (Fabri-Ruiz et al., 2019; Guillaumot et al., 2019). In this context, modeling species distribution remains challenging and therefore the present study proposes a new framework by using statistical modeling chain approach to improve environmental data and obtain consistent predictors for EHM in coastal areas. This approach for modeling and projecting harmful algal species could: i) inform the environmental conditions / variation may favor HABs occurrence; ii) assist scientists and stakeholders to design and implement effective future monitoring programs, iii) help to identify regions that are particularly sensitive to HABs and therefore help to develop warning systems adapted to future climate conditions, iv) design strategies to minimise anthropogenic pressures in the coastal environments and thus

prevent the occurrence of disruptive HAB events in the near future.

4.7. Limitations and future research needed

The study does not take into account the various sources of uncertainty in projecting changes in environmental data due to the numerical cost of the modeling chain used. These include uncertainty in model choice, uncertainty in natural variability and uncertainty in socioeconomic scenarios. It is therefore acknowledged that the study examines only one of many possible future climate and biological scenarios. The study does not claim to predict the future, but rather explores the methodological approach to linking global climate change with changes in species abundance, taking into account their biology and ecology.

Several limitations are associated with using EHMs to study climate change impacts. These models do not provide direct causal links between environmental parameters and species abundance (Dormann et al., 2012; Fabri-Ruiz et al., 2021). They do not explicitly account for the underlying processes that influence these response variables, and lack explicit integration of demographic processes and biotic interactions, and as a result EHMs have often struggled with limited ability to accurately extrapolate across different spatial and temporal contexts (Elith et al., 2010; Guillaumot et al., 2020). In contrast, mechanistic models may offer more realistic predictions and greater potential for transferability, as they are based on parameters of species responses to environmental conditions derived from experimental data. Although mechanistic models appear to be more effective at defining species' fundamental niches, they are also susceptible to provide inaccurate prediction (Fabri-Ruiz et al., 2021; Yates et al., 2018) and their use has so far been restricted to a few well-studied taxa (Buckley et al., 2011; Evans et al., 2015; Thomas and Bacher, 2018). An interesting approach for further investigation of the present study could be the combination of a correlative and a mechanistic model using a Bayesian framework (Guillaumot et al., 2022). The mechanistic model could be based on the Cardinal Temperature Model with Inflection that describes how an organism's growth, development, or other physiological processes respond to temperature. It incorporates an inflection point, which represents the temperature at which the rate of growth or development changes direction, typically from increasing to decreasing. Ecophysiological studies led on *Ostreopsis* could be used to build this model (Drouet et al., 2024). The combination of the correlative and mechanistic model in a hybrid approach could exploit the strengths of both models to improve the accuracy of estimating the potential ecological species habitat (Castro et al., 2020; Fabri-Ruiz et al., 2021; Kearney and Porter, 2009; Pertierra et al., 2020).

5. Conclusion

This study represents a significant step forward in comprehending the potential impact of climate change on the spatial-temporal distribution of *Ostreopsis* cf. *ovata* blooms in the Western Mediterranean Sea. By employing a robust ecological habitat model integrated with high-resolution climate change simulations under the RCP8.5 scenario, the study emphasized the importance of environmental factors, such as temperature, salinity, and inorganic nutrient concentrations, that influence *O. cf. ovata* abundances. While the overall intensity of blooms might not see significant changes, the study reveals two important trends: i) blooms are likely to begin earlier and last longer into the year, and ii) there will be noticeable differences in bloom patterns across the Western Mediterranean Sea. Such changes in bloom dynamics pose potential risks to marine ecosystems, public health, and economic activities due to the toxic nature of *O. cf. ovata*. The results highlight the usefulness of ecological habitat models within a strong statistical framework for providing precise predictions, and they underline the importance of regular monitoring sampling program to develop more informed and accurate forecasts regarding the future state of marine environment, in particular regarding HABs.

CRediT authorship contribution statement

S. Fabri-Ruiz: Writing – review & editing, Writing – original draft, Visualization, Validation, Software, Resources, Methodology, Investigation, Formal analysis, Data curation, Conceptualization. **E. Berdalet:** Writing – review & editing, Writing – original draft, Investigation, Data curation. **C. Ulses:** Writing – review & editing, Writing – original draft, Methodology, Formal analysis, Data curation. **S. Somot:** Writing – review & editing, Writing – original draft, Methodology, Investigation, Formal analysis, Data curation. **M. Vila:** Writing – review & editing, Writing – original draft, Data curation. **R. Lemée:** Writing – review & editing, Writing – original draft, Validation, Supervision, Project administration, Methodology, Investigation, Funding acquisition, Formal analysis, Data curation, Conceptualization. **J.-O. Irisson:** Writing – review & editing, Writing – original draft, Visualization, Validation, Supervision, Software, Resources, Project administration, Methodology, Investigation, Funding acquisition, Formal analysis, Data curation, Conceptualization.

Declaration of competing interest

The authors declare no conflict of interest.

Data availability

All the data used (environmental and biological data) and the scripts for processing environmental data, fitting ecological habitat models, and producing the figures in this manuscript are available here: <https://datadryad.org/stash/dataset/doi:10.5061/dryad.44j0zpcn5> and noted in the manuscript. The raw data from the CNRM-RCSM4 historical and scenario simulations are openly available, after registration, on the Med-CORDEX centralized database in netCDF format (<https://www.medcordex.eu/medcordex.php>). Help to handle them can be requested at contact.cordex@meteo.fr. The raw data from the Eco3M-S biogeochemical simulation can be accessed on request to caroline.uls@univ-tlse3.fr. The reanalysis fields are openly available from Copernicus <https://marine.copernicus.eu/access-data>. The environmental monitoring stations data is openly available from SOMLIT <https://www.somlit.fr/demande-de-donnees/>.

Acknowledgements

This study was supported by the project CoCliME (a part of ERA4CS, an ERA-NET initiated by JPI Climate, and funded by EPA -Ireland-, ANR -France-, BMBF -Germany-, UEFISCDI -Romania-, RCN -Norway- and FORMAS -Sweden-, with co-funding by the European Union; Grant 6904462). Funds were also granted by the Spanish government through the OSTREORISK project (CTM2014-53818-R) and the 'Severo Ochoa Centre of Excellence' accreditation (CEX2019-000928-S). The monitoring of *Ostreopsis* in Monaco was supported by the "Direction de l'Environnement de Monaco". The regional climate simulations used in this study are part of the CNRM contribution to the Med-CORDEX initiative (www.medcordex.eu) and are available in this framework. The authors thank F. Sevault for developing and running the CNRM-RCSM4 model and for preparing and sharing the model outputs.

Contributions

S. Fabri-Ruiz, J.-O. Irisson and R. Lemée conceived the idea and designed the manuscript. C. Ulses, S. Somot, provided historical and future physical and biogeochemical data. S. Fabri-Ruiz and J.-O. Irisson provided and analyzed the data. E. Berdalet and M. Vila provided *Ostreopsis* blooms data from Llavanneres. R. Lemée provided *Ostreopsis* data from France and Monaco. All authors equally contributed to the interpretation of analyses. S. F. R. wrote the manuscript with contributions and input from all authors.

Appendix A. Supplementary data

Supplementary data to this article can be found online at <https://doi.org/10.1016/j.scitotenv.2024.174726>.

References

- Accoroni, S., Totti, C., 2016. The toxic benthic dinoflagellates of the genus *Ostreopsis* in temperate areas: a review. *Adv. Oceanogr. Limnol.* 7, 1–15. <https://doi.org/10.4081/aiol.2016.5591>.
- Accoroni, S., Romagnoli, T., Colombo, F., Pennesi, C., Di Camillo, C.G., Marini, M., Battocchi, C., Ciminiello, P., Dell'Aversano, C., Dello Iacovo, E., Fattorusso, E., Tartaglione, L., Penna, A., Totti, C., 2011. *Ostreopsis* cf. *ovata* bloom in the northern Adriatic Sea during summer 2009: ecology, molecular characterization and toxin profile. *Mar. Pollut. Bull.* 62, 2512–2519. <https://doi.org/10.1016/j.marpolbul.2011.08.003>.
- Accoroni, S., Romagnoli, T., Pichierrri, S., Totti, C., 2014. New insights on the life cycle stages of the toxic benthic dinoflagellate *Ostreopsis* cf. *ovata*. *Harmful Algae* 34, 7–16. <https://doi.org/10.1016/j.hal.2014.02.003>.
- Accoroni, S., Glibert, P.M., Pichierrri, S., Romagnoli, T., Marini, M., Totti, C., 2015. A conceptual model of annual *Ostreopsis* cf. *ovata* blooms in the northern Adriatic Sea based on the synergic effects of hydrodynamics, temperature, and the N:P ratio of water column nutrients. *Harmful Algae* 45, 14–25. <https://doi.org/10.1016/j.hal.2015.04.002>.
- Adachi, S.A., Nishizawa, S., Ando, K., Yamaura, T., Yoshida, R., Yashiro, H., Kajikawa, Y., Tomita, H., 2019. An evaluation method for uncertainties in regional climate projections. *Atmos. Sci. Lett.* 20, e877. <https://doi.org/10.1002/asl.877>.
- Amzil, Z., Sibat, M., Chomerat, N., Grossel, H., Marco-Miralles, F., Lemee, R., Nezan, E., Sechet, V., 2012. Ovatoxin-a and palytoxin accumulation in seaweed in relation to *Ostreopsis* cf. *ovata* blooms on the French Mediterranean Coast. *Mar. Drugs* 10, 477–496. <https://doi.org/10.3390/md10020477>.
- Anderson, D.M., Cembella, A.D., Hallegraeff, G.M., 2012. Progress in understanding harmful algal blooms: paradigm shifts and new technologies for research, monitoring, and management. *Annu. Rev. Mar. Sci.* 4, 143–176. <https://doi.org/10.1146/annurev-marine-120308-081121>.
- Araújo, M.B., Guisan, A., 2006. Five (or so) challenges for species distribution modelling. *J. Biogeogr.* 33, 1677–1688. <https://doi.org/10.1111/j.1365-2699.2006.01584.x>.
- Asnaghi, V., Pecorino, D., Ottaviani, E., Pedroncini, A., Bertolotto, R.M., Chiantore, M., 2017. A novel application of an adaptable modeling approach to the management of toxic microalgal bloom events in coastal areas. *Harmful Algae* 63, 184–192. <https://doi.org/10.1016/j.hal.2017.02.003>.
- Benedetti, F., Guilhaumon, F., Adloff, F., Ayata, S., 2018. Investigating uncertainties in zooplankton composition shifts under climate change scenarios in the Mediterranean Sea. *Ecography* 41, 345–360. <https://doi.org/10.1111/ecog.02434>.
- Bensoussan, N., Paireaud, I., Garreau, P., Somot, S., Garrabou, J., 2013. Multidisciplinary Approach to Assess Potential Risk of Mortality of Benthic Ecosystems Facing Climate Change in the NW Mediterranean Sea.
- Berdalet, E., Tester, P.A., Chinain, M., Fraga, S., Lemée, R., Litaker, W., Penna, A., Usup, G., Vila, M., Zingone, A., 2017. Harmful algal blooms in benthic systems: recent progress and future research. *Oceanography* 30, 36–45.
- Berdalet, E., Pavau, A.-S., Abós-Herrándiz, R., Travers, M., Appéré, G., Vila, M., Thomas, J., De Haro, L., Estrada, M., Medina-Pérez, N.I., Viure, L., Karlson, B., Lemée, R., 2022. Environmental, human health and socioeconomic impacts of *Ostreopsis* spp. blooms in the NW Mediterranean. *Harmful Algae* 119, 102320. <https://doi.org/10.1016/j.hal.2022.102320>.
- Beygelzimer, A., Kakadet, S., Langford, J., Arya, S., Mount, D., Li, S., Li, M.S., 2024. Package FNN: fast nearest neighbor search algorithms and applications. R package version 1.1.3. <https://CRAN.R-project.org/package=FNN> [WWW Document].
- Biré, R., Trotereau, S., Lemée, R., Delpont, C., Chabot, B., Aumond, Y., Krys, S., 2013. Occurrence of palytoxins in marine organisms from different trophic levels of the French Mediterranean coast harvested in 2009. *Harmful Algae* 28, 10–22. <https://doi.org/10.1016/j.hal.2013.04.007>.
- Biré, R., Trotereau, S., Lemée, R., Oregioni, D., Delpont, C., Krys, S., Guérin, T., 2015. Hunt for palytoxins in a wide variety of marine organisms harvested in 2010 on the French Mediterranean coast. *Mar. Drugs* 13, 5425–5446. <https://doi.org/10.3390/md13085425>.
- Brissard, C., Herrenknecht, C., Séchet, V., Hervé, F., Pisapia, F., Harcouet, J., Lémée, R., Chomérat, N., Hess, P., Amzil, Z., 2014. Complex toxin profile of French Mediterranean *Ostreopsis* cf. *ovata* strains, seaweed accumulation and ovatoxins depurification. *Mar. Drugs* 12, 2851–2876. <https://doi.org/10.3390/md12052851>.
- Buckley, L.B., Waaser, S.A., MacLean, H.J., Fox, R., 2011. Does including physiology improve species distribution model predictions of responses to recent climate change? *Ecology* 92, 2214–2221. <https://doi.org/10.1890/11-0066.1>.
- Burrows, M.T., Schoeman, D.S., Buckley, L.B., Moore, P., Poloczanska, E.S., Brander, K.M., Brown, C., Bruno, J.F., Duarte, C.M., Halpern, B.S., Holding, J., Kappel, C.V., Kiessling, W., O'Connor, M.L., Pandolfi, J.M., Parmesan, C., Schwing, F.B., Sydeman, W.J., Richardson, A.J., 2011. The pace of shifting climate in marine and terrestrial ecosystems. *Science* 334, 652–655. <https://doi.org/10.1126/science.1210288>.
- Carnicer, O., Guallar, C., Andree, K.B., Diogène, J., Fernández-Tejedor, M., 2015. *Ostreopsis* cf. *ovata* dynamics in the NW Mediterranean Sea in relation to biotic and abiotic factors. *Environ. Res.* 143, 89–99. <https://doi.org/10.1016/j.envres.2015.08.023>.
- Carnicer, O., García-Altres, M., Andree, K.B., Tartaglione, L., Dell'Aversano, C., Ciminiello, P., De La Iglesia, P., Diogène, J., Fernández-Tejedor, M., 2016. *Ostreopsis* cf. *ovata* from western Mediterranean Sea: physiological responses under different temperature and salinity conditions. *Harmful Algae* 57, 98–108. <https://doi.org/10.1016/j.hal.2016.06.002>.
- Castro, L.C., Cetina-Heredia, P., Roughan, M., Dworjany, S., Thibaut, L., Chamberlain, M.A., Feng, M., Vergés, A., 2020. Combined mechanistic modelling predicts changes in species distribution and increased co-occurrence of a tropical urchin herbivore and a habitat-forming temperate kelp. *Divers. Distrib.* 26, 1211–1226. <https://doi.org/10.1111/ddi.13073>.
- Chang, F.H., Shimizu, Y., Hay, B., Stewart, R., Mackay, G., Tasker, R., 2000. Three recently recorded *Ostreopsis* spp. (Dinophyceae) in New Zealand: temporal and regional distribution in the upper North Island from 1995 to 1997. *N. Z. J. Mar. Freshw. Res.* 34, 29–39. <https://doi.org/10.1080/00288330.2000.9516913>.
- Chen, T., Guestrin, C., 2016. XGBoost: a scalable tree boosting system. In: Proceedings of the 22nd ACM SIGKDD International Conference on Knowledge Discovery and Data Mining. Presented at the KDD '16: The 22nd ACM SIGKDD International Conference on Knowledge Discovery and Data Mining, ACM, San Francisco California USA, pp. 785–794. <https://doi.org/10.1145/2939672.2939785>.
- Cheung, W.W.L., Lam, V.W.Y., Sarmiento, J.L., Kearney, K., Watson, R., Pauly, D., 2009. Projecting global marine biodiversity impacts under climate change scenarios. *Fish. Fish.* 10, 235–251. <https://doi.org/10.1111/j.1467-2979.2008.00315.x>.
- Ciminiello, P., Dell'Aversano, C., Iacovo, E.D., Fattorusso, E., Forino, M., Tartaglione, L., Yasumoto, T., Battocchi, C., Giacobbe, M., Amorim, A., Penna, A., 2013. Investigation of toxin profile of Mediterranean and Atlantic strains of *Ostreopsis* cf. *siamensis* (Dinophyceae) by liquid chromatography–high resolution mass spectrometry. *Harmful Algae* 23, 19–27. <https://doi.org/10.1016/j.hal.2012.12.002>.
- Ciminiello, P., Dell'Aversano, C., Iacovo, E.D., Fattorusso, E., Forino, M., Tartaglione, L., Benedettini, G., Onorari, M., Serena, F., Battocchi, C., Casabianca, S., Penna, A., 2014. First finding of *Ostreopsis* cf. *ovata* toxins in marine aerosols. *Environ. Sci. Technol.* 48, 3532–3540. <https://doi.org/10.1021/es405617d>.
- Cohu, S., Thibaut, T., Mangialajo, L., Labat, J.-P., Passafiume, O., Blanfuné, A., Simon, N., Cottalorda, J.-M., Lemée, R., 2011. Occurrence of the toxic dinoflagellate *Ostreopsis* cf. *ovata* in relation with environmental factors in Monaco (NW Mediterranean). *Mar. Pollut. Bull.* 62, 2681–2691. <https://doi.org/10.1016/j.marpolbul.2011.09.022>.
- Cohu, S., Mangialajo, L., Thibaut, T., Blanfuné, A., Marro, S., Lemée, R., 2013. Proliferation of the toxic dinoflagellate *Ostreopsis* cf. *ovata* in relation to depth, biotic substrate and environmental factors in the North West Mediterranean Sea. *Harmful Algae* 24, 32–44. <https://doi.org/10.1016/j.hal.2013.01.002>.
- Cossarini, G., Feudale, L., Teruzzi, A., Bolzon, G., Coidessa, G., Solidoro, C., Di Biagio, V., Amadio, C., Lazzari, P., Brosich, A., Salon, S., 2021. High-resolution reanalysis of the Mediterranean Sea biogeochemistry (1999–2019). *Front. Mar. Sci.* 8, 741486. <https://doi.org/10.3389/fmars.2021.741486>.
- Darmaraki, S., Somot, S., Sevault, F., Nabat, P., Cabos Narvaez, W.D., Cavicchia, L., Djurdjevic, V., Li, L., Sannino, G., Sein, D.V., 2019. Future evolution of marine heatwaves in the Mediterranean Sea. *Clim. Dyn.* 53, 1371–1392. <https://doi.org/10.1007/s00382-019-04661-z>.
- Doney, S.C., Ruckelshaus, M., Emmett Duffy, J., Barry, J.P., Chan, F., English, C.A., Galindo, H.M., Grebmeier, J.M., Hollowed, A.B., Knowlton, N., Polovina, J., Rabalais, N.N., Sydeman, W.J., Talley, L.D., 2012. Climate change impacts on marine ecosystems. *Annu. Rev. Mar. Sci.* 4, 11–37. <https://doi.org/10.1146/annurev-marine-041911-111611>.
- Dormann, C.F., Schymanski, S.J., Cabral, J., Chuine, I., Graham, C., Hartig, F., Kearney, M., Morin, X., Römermann, C., Schröder, B., Singer, A., 2012. Correlation and process in species distribution models: bridging a dichotomy. *J. Biogeogr.* 39, 2119–2131. <https://doi.org/10.1111/j.1365-2699.2011.02659.x>.
- Dormann, C.F., Elith, J., Bacher, S., Buchmann, C., Carl, G., Carré, G., Marquéz, J.R.G., Gruber, B., Lafourcade, B., Leitão, P.J., Münkemüller, T., McClean, C., Osborne, P.E., Reineking, B., Schröder, B., Skidmore, A.K., Zurell, D., Lautenbach, S., 2013. Collinearity: a review of methods to deal with it and a simulation study evaluating their performance. *Ecography* 36, 27–46. <https://doi.org/10.1111/j.1600-0587.2012.07348.x>.
- Drouet, K., Jauzein, C., Herviot-Heath, D., Hariri, S., Laza-Martinez, A., Lecadet, C., Plus, M., Seoane, S., Sourisseau, M., Lemée, R., Siano, R., 2021. Current distribution and potential expansion of the harmful benthic dinoflagellate *Ostreopsis* cf. *siamensis* towards the warming waters of the Bay of Biscay, North-East Atlantic. *Environ. Microbiol.* 23, 4956–4979. <https://doi.org/10.1111/1462-2920.15406>.
- Drouet, K., Jauzein, C., Gasparini, S., Pavau, A.-S., Berdalet, E., Marro, S., Davenet-Sbirrazioli, V., Siano, R., Lemée, R., 2022. The benthic toxic dinoflagellate *Ostreopsis* cf. *ovata* in the NW Mediterranean Sea: relationship between sea surface temperature and bloom phenology. *Harmful Algae* 112, 102184. <https://doi.org/10.1016/j.hal.2022.102184>.
- Drouet, K., Lemée, R., Guilloud, E., Schmitt, S., Laza-Martinez, A., Seoane, S., Boutoute, M., Réveillon, D., Hervé, F., Siano, R., Jauzein, C., 2024. Ecophysiological responses of *Ostreopsis* towards temperature: a case study of benthic HAB facing ocean warming. *Harmful Algae* 135, 102648. <https://doi.org/10.1016/j.hal.2024.102648>.
- Durando, P., Ansaldi, F., Oreste, P., Moscatelli, P., Marensi, L., Grillo, C., Gasparini, R., Icardi, G., Surveillance, C.G. for the L.S.A., 2007. *Ostreopsis ovata* and human health: epidemiological and clinical features of respiratory syndrome outbreaks from a two-year syndromic surveillance, 2005–06, in north-west Italy. *In: Weekly Releases (1997–2007)*, 12, p. 3212.

- Edwards, M., Richardson, A.J., 2004. Impact of climate change on marine pelagic phenology and trophic mismatch. *Nature* 430, 881–884. <https://doi.org/10.1038/nature02808>.
- Elith, J., Leathwick, J.R., 2009. Species distribution models: ecological explanation and prediction across space and time. *Annu. Rev. Ecol. Evol. Syst.* 40, 677–697. <https://doi.org/10.1146/annurev.ecolsys.110308.120159>.
- Elith, J., Leathwick, J.R., Hastie, T., 2008. A working guide to boosted regression trees. *J. Anim. Ecol.* 77, 802–813. <https://doi.org/10.1111/j.1365-2656.2008.01390.x>.
- Elith, J., Kearney, M., Phillips, S., 2010. The art of modelling range-shifting species. *Methods Ecol. Evol.* 1, 330–342.
- Ellwood, N., Pasella, M., Totti, C., Accoroni, S., 2020. Growth and phosphatase activities of *Ostreopsis cf. ovata* biofilms supplied with diverse dissolved organic phosphorus (DOP) compounds. *Aquat. Microb. Ecol.* 85, 155–166. <https://doi.org/10.3354/ame01946>.
- Erdner, D.L., Dyble, J., Parsons, M.L., Stevens, R.C., Hubbard, K.A., Wrabel, M.L., Moore, S.K., Lefebvre, K.A., Anderson, D.M., Bienfang, P., Bidigare, R.R., Parker, M. S., Moeller, P., Brand, L.E., Trainer, V.L., 2008. Centers for oceans and human health: a unified approach to the challenge of harmful algal blooms. *Environ. Health* 7, S2. <https://doi.org/10.1186/1476-069X-7-S2-S2>.
- Evans, T.G., Diamond, S.E., Kelly, M.W., 2015. Mechanistic species distribution modelling as a link between physiology and conservation. *Conserv. Physiol.* 3, cov056 <https://doi.org/10.1093/conphys/cov056>.
- Fabri-Ruiz, S., Danis, B., David, B., Saucède, T., 2019. Can we generate robust species distribution models at the scale of the Southern Ocean? *Divers. Distrib.* 25, 21–37.
- Fabri-Ruiz, S., Guillaumot, C., Agüera, A., Danis, B., Saucède, T., 2021. Using correlative and mechanistic niche models to assess the sensitivity of the Antarctic echinoid *Sterechinus neumayeri* to climate change. *Polar Biol.* 44, 1517–1539. <https://doi.org/10.1007/s00300-021-02886-5>.
- Faimali, M., Giussani, V., Piazza, V., Garaventa, F., Corrà, C., Asnaghi, V., Privitera, D., Gallus, L., Cattaneo-Vietti, R., Mangialajo, L., Chiantore, M., 2012. Toxic effects of harmful benthic dinoflagellate *Ostreopsis ovata* on invertebrate and vertebrate marine organisms. *Mar. Environ. Res.* 76, 97–107. <https://doi.org/10.1016/j.marenvres.2011.09.010>.
- Friedman, J.H., 2001. Greedy function approximation: a gradient boosting machine. *Ann. Stat.* 29, 1189–1232. <https://doi.org/10.1214/aos/1013203451>.
- Fukuy, Y., 1981. Taxonomical study on benthic dinoflagellates collected in coral reefs. *Bull. Jpn. Soc. Sci. Fish.* 47, 967–978. <https://doi.org/10.2331/suisan.47.967>.
- Gallitelli, M., Ungaro, N., Addante, L.M., Procacci, V., Silver, N.G., Sabbà, C., 2005. Respiratory illness as a reaction to tropical algal blooms occurring in a temperate climate. *Jama* 293, 2595–2600.
- Gattuso, J.-P., Magnan, A., Billé, R., Cheung, W.W.L., Howes, E.L., Joos, F., Allemand, D., Bopp, L., Cooley, S.R., Eakin, C.M., Hoegh-Guldberg, O., Kelly, R.P., Pörtner, H.-O., Rogers, A.D., Baxter, J.M., Laffoley, D., Osborn, D., Rankovic, A., Rochette, J., Sumaila, U.R., Treyer, S., Turley, C., 2015. Contrasting futures for ocean and society from different anthropogenic CO₂ emissions scenarios. *Science* 349, aac4722. <https://doi.org/10.1126/science.aac4722>.
- Gelman, A., Hill, J., 2006. *Data Analysis Using Regression and Multilevel/Hierarchical Models*. Cambridge University Press.
- Gémin, M.-P., Réveillon, D., Hervé, F., Pavaux, A.-S., Tharaud, M., Séchet, V., Bertrand, S., Lemée, R., Amzil, Z., 2020. Toxin content of *Ostreopsis cf. ovata* depends on bloom phases, depth and macroalgal substrate in the NW Mediterranean Sea. *Harmful Algae* 92, 101727. <https://doi.org/10.1016/j.hal.2019.101727>.
- Giorgi, F., 2006. Climate change hot-spots. *Geophys. Res. Lett.* 33, 2006GL025734 <https://doi.org/10.1029/2006GL025734>.
- Glibert, P.M., Icarus Allen, J., Artioli, Y., Beusen, A., Bouwman, L., Harle, J., Holmes, R., Holt, J., 2014. Vulnerability of coastal ecosystems to changes in harmful algal bloom distribution in response to climate change: projections based on model analysis. *Glob. Chang. Biol.* 20, 3845–3858. <https://doi.org/10.1111/gcb.12662>.
- Gobler, C.J., Doherty, O.M., Hattenrath-Lehmann, T.K., Griffith, A.W., Kang, Y., Litaker, R.W., 2017. Ocean warming since 1982 has expanded the niche of toxic algal blooms in the North Atlantic and North Pacific oceans. *Proc. Natl. Acad. Sci. U. S. A.* 114, 4975–4980. <https://doi.org/10.1073/pnas.1619575114>.
- Gomes, V.H.F., Ijff, S.D., Raes, N., Amaral, I.L., Salomão, R.P., De Souza Coelho, L., De Almeida Matos, F.D., Castilho, C.V., De Andrade Lima Filho, D., López, D.C., Guevara, J.E., Magnusson, W.E., Phillips, O.L., Wittmann, F., De Jesus Veiga Carim, M., Martins, M.P., Irueme, M.V., Sabatier, D., Molino, J.-F., Bánki, O.S., Da Silva Guimarães, J.R., Pitman, N.C.A., Piedade, M.T.F., Mendoza, A.M., Luize, B.G., Venticinque, E.M., De Leão Novo, E.M.M., Vargas, P.N., Silva, T.S.F., Manzatto, A.G., Terborgh, J., Reis, N.F.C., Montero, J.C., Casula, K.R., Marimon, B.S., Marimon, B.-H., Coronado, E.N.H., Feldpausch, T.R., Duque, A., Zartman, C.E., Arboleda, N.C., Killeen, T.J., Mostacedo, B., Vasquez, R., Schöngart, J., Assis, R.L., Medeiros, M.B., Simon, M.F., Andrade, A., Laurance, W.F., Camargo, J.L., Demarchi, L.O., Laurance, S.G.W., De Sousa Farias, E., Nascimento, H.E.M., Revilla, J.D.C., Quaresma, A., Costa, F.R.C., Vieira, I.C.G., Cintra, B.B.L., Castellanos, H., Brienen, R., Stevenson, P.R., Feitosa, Y., Duivenvoorden, J.F., Aymard, C., G.A., Mogollón, H.F., Targhetta, N., Comiskey, J.A., Vicentini, A., Lopes, A., Damasco, G., Dávila, N., García-Villacorta, R., Levis, C., Schiatti, J., Souza, P., Emilio, T., Alonzo, A., Neill, D., Dallmeier, F., Ferreira, L.V., Araujo-Murakami, A., Praia, D., Do Amaral, D.D., Carvalho, F.A., De Souza, F.C., Feeley, K., Arroyo, L., Pansonato, M.P., Gribel, R., Villa, B., Licona, J.C., Fine, P.V.A., Cerón, C., Baraloto, C., Jimenez, E.M., Stropp, J., Engel, J., Silveira, M., Mora, M.C.P., Petronelli, P., Maas, P., Thomas-Caesar, R., Henkel, T.W., Daly, D., Paredes, M.R., Baker, T.R., Fuentes, A., Peres, C. A., Chave, J., Pena, J.L.M., Dexter, K.G., Silman, M.R., Jørgensen, P.M., Pennington, T., Di Fiore, A., Valverde, F.C., Phillips, J.F., Rivas-Torres, G., Von Hildebrand, P., Van Andel, T.R., Ruschel, A.R., Prieto, A., Rudas, A., Hoffman, B., Vela, C.I.A., Barbosa, E.M., Zent, E.L., Gonzales, G.P.G., Doza, H.P.D., De Andrade Miranda, I.P., Guillaumet, J.-L., Pinto, L.F.M., De Matos Bonates, L.C., Silva, N., Gómez, R.Z., Zent, S., Gonzales, T., Vos, V.A., Malhi, Y., Oliveira, A.A., Cano, A., Albuquerque, B.W., Vriesendorp, C., Correa, D.F., Torre, E.V., Van Der Heijden, G., Ramirez-Angulo, H., Ramos, J.F., Young, K.R., Rocha, M., Nascimento, M.T., Medina, M.N.U., Tirado, M., Wang, O., Sierra, R., Torres-Lezama, A., Mendoza, C., Ferreira, C., Baider, C., Villarroel, D., Balslev, H., Mesones, I., Giraldo, L.E.U., Casas, L.F., Reategui, M.A.A., Linares-Palomino, R., Zagt, R., Cárdenas, S., Farfan-Rios, W., Sampaio, A.F., Pauletto, D., Sandoval, E.H.V., Arevalo, F.R., Huamantupa-Chuquimaco, I., Garcia-Cabrera, K., Hernandez, L., Gamarra, L.V., Alexiades, M.N., Pansini, S., Cuenca, W.P., Milliken, W., Ricardo, J., Lopez-Gonzalez, G., Pos, E., Ter Steege, H., 2018. Species distribution modelling: contrasting presence-only models with plot abundance data. *Sci. Rep.* 8, 1003. <https://doi.org/10.1038/s41598-017-18927-1>.
- Orbici, S., Avio, G.C., Benedetti, M., Totti, C., Accoroni, S., Pichierrri, S., Bacchiocchi, S., Orletti, R., Graziosi, T., Regoli, F., 2013. Effects of harmful dinoflagellate *Ostreopsis cf. ovata* exposure on immunological, histological and oxidative responses of mussels *Mytilus galloprovincialis*. *Fish Shellfish Immunol.* 35, 941–950. <https://doi.org/10.1016/j.fsi.2013.07.003>.
- Granéli, E., Vidyaratna, N.K., Funari, E., Cumarantunga, P.R.T., Scenati, R., 2011. Can increases in temperature stimulate blooms of the toxic benthic dinoflagellate *Ostreopsis ovata*? *Harmful Algae* 10, 165–172. <https://doi.org/10.1016/j.hal.2010.09.002>.
- Greenwell, B.M., 2017. pdp: An R Package for Constructing Partial Dependence Plots. *The R Journal* 9, 421. <https://doi.org/10.32614/RJ-2017-016>.
- Guerrini, F., Pezzolesi, L., Feller, A., Riccardi, M., Ciminiello, P., Dell’Aversano, C., Tartaglione, L., Iacovo, E.D., Fattorusso, E., Forino, M., Pistocchi, R., 2010. Comparative growth and toxin profile of cultured *Ostreopsis ovata* from the Tyrrhenian and Adriatic Seas. *Toxicol.* 55, 211–220. <https://doi.org/10.1016/j.toxicol.2009.07.019>.
- Guidi-Guilvard, L.D., Gasparini, S., Lemée, R., 2012. The negative impact of *Ostreopsis cf. Ovata* on phytal meiofauna from the coastal NW Mediterranean. *Cryptogam. Algol.* 33, 121–128. <https://doi.org/10.7872/crya.v33.iss2.2011.121>.
- Guillaumot, C., Moreau, C., Danis, B., Saucède, T., 2020. Extrapolation in species distribution modelling. Application to Southern Ocean marine species. *Prog. Oceanogr.* 188, 102438 <https://doi.org/10.1016/j.pocean.2020.102438>.
- Guillaumot, C., Artois, J., Saucède, T., Demoustier, L., Moreau, C., Eléaume, M., Agüera, A., Danis, B., 2019. Broad-scale species distribution models applied to data-poor areas. *Prog. Oceanogr.* 175, 198–207. <https://doi.org/10.1016/j.pocean.2019.04.007>.
- Guillaumot, C., Belmaker, J., Buba, Y., Fourcy, D., Dubois, P., Danis, B., Le Moan, E., Saucède, T., 2022. Classic or hybrid? The performance of next generation ecological models to study the response of Southern Ocean species to changing environmental conditions. *Divers. Distrib.* 28, 2286–2302. <https://doi.org/10.1111/ddi.13617>.
- Guisan, A., Thuiller, W., 2005. Predicting species distribution: offering more than simple habitat models. *Ecol. Lett.* 8, 993–1009. <https://doi.org/10.1111/j.1461-0248.2005.00792.x>.
- Guisan, A., Zimmermann, N.E., 2000. Predictive habitat distribution models in ecology. *Ecol. Model.* 135, 147–186. [https://doi.org/10.1016/S0304-3800\(00\)00354-9](https://doi.org/10.1016/S0304-3800(00)00354-9).
- Hoagland, P., Scatista, S., 2006. The economic effects of harmful algal blooms. In: *Ecology of Harmful Algae*, pp. 391–402.
- Hoegh-Guldberg, O., Bruno, J.F., 2010. The impact of climate change on the world’s marine ecosystems. *Science* 328, 1523–1528. <https://doi.org/10.1126/science.1189930>.
- Howard, C., Stephens, P.A., Pearce-Higgins, J.W., Gregory, R.D., Willis, S.G., 2014. Improving species distribution models: the value of data on abundance. *Methods Ecol. Evol.* 5, 506–513. <https://doi.org/10.1111/2041-210X.12184>.
- IPCC, 2023. Climate change 2023: synthesis report. In: Core Writing Team, Lee, H., Romero, J. (Eds.), Contribution of Working Groups I, II and III to the Sixth Assessment Report of the Intergovernmental Panel on Climate Change. IPCC, Geneva, Switzerland, pp. 35–115. <https://doi.org/10.59327/IPCC/AR6-9789291691647IPCC>.
- Italiano, A., Di Cioccio, D., Borra, M., Biffali, E., Procacci, G., Zingone, A., 2014. AFLP reveals intrinsic variations in geographically diverse *Ostreopsis cf. ovata* populations. In: *Proceedings of the 15th International Conference on Harmful Algae*. Jauzein, C., Açaf, L., Accoroni, S., Asnaghi, V., Fricke, A., Hachani, M.A., Abboud-Abi Saab, M., Chiantore, M., Mangialajo, L., Totti, C., Zaghmouri, I., Lemée, R., 2018. Optimization of sampling, cell collection and counting for the monitoring of benthic harmful algal blooms: application to *Ostreopsis* spp. blooms in the Mediterranean Sea. *Ecol. Indic.* 91, 116–127. <https://doi.org/10.1016/j.ecolind.2018.03.089>.
- Kearney, M., Porter, W., 2009. Mechanistic niche modelling: combining physiological and spatial data to predict species’ ranges. *Ecol. Lett.* 12, 334–350. <https://doi.org/10.1111/j.1461-0248.2008.01277.x>.
- Kouakou, C.R.C., Poder, T.G., 2019. Economic impact of harmful algal blooms on human health: a systematic review. *J. Water Health* 17, 499–516. <https://doi.org/10.2166/wh.2019.064>.
- Liu, C., Newell, G., White, M., 2016. On the selection of thresholds for predicting species occurrence with presence-only data. *Ecol. Evol.* 6, 337–348.
- Mabrouk, L., Hamza, A., Brahim, M.B., Bradai, M.-N., 2011. Temporal and depth distribution of microepiphytes on *Posidonia oceanica* (L.) Delile leaves in a meadow off Tunisia: temporal and depth distribution of microepiphytes. *Mar. Ecol.* 32, 148–161. <https://doi.org/10.1111/j.1439-0485.2011.00432.x>.
- Mangialajo, L., Bertolotto, R., Cattaneo-Vietti, R., Chiantore, M., Grillo, C., Lemée, R., Melchiorre, N., Moretto, P., Povero, P., Ruggieri, N., 2008. The toxic benthic dinoflagellate *Ostreopsis ovata*: quantification of proliferation along the coastline of Genoa, Italy. *Mar. Pollut. Bull.* 56, 1209–1214. <https://doi.org/10.1016/j.marpollbul.2008.02.028>.

- Mangialajo, L., Ganzin, N., Accoroni, S., Asnaghi, V., Blanfuné, A., Cabrini, M., Cattaneo-Vietti, R., Chavanon, F., Chiantore, M., Cohu, S., Costa, E., Fornasaro, D., Grosseil, H., Marco-Miralles, F., Masó, M., René, A., Rossi, A.M., Sala, M.M., Thibaut, T., Totti, C., Vila, M., Lemée, R., 2011. Trends in *Ostreopsis* proliferation along the Northern Mediterranean coasts. *Toxicon* 57, 408–420. <https://doi.org/10.1016/j.toxicon.2010.11.019>.
- Mangialajo, L., Fricke, A., Perez-Gutierrez, G., Catania, D., Jauzein, C., Lemee, R., 2017. Benthic dinoflagellate integrator (BEDI): a new method for the quantification of benthic harmful algal blooms. *Harmful Algae* 64, 1–10. <https://doi.org/10.1016/j.hal.2017.03.002>.
- Medina-Pérez, N.I., Cerdán-García, E., Rubió, F., Viure, L., Estrada, M., Moyano, E., Berdalet, E., 2023. Progress on the link between nutrient availability and toxin production by *Ostreopsis* cf. *ovata*: field and laboratory experiments. *Toxins* 15, 188. <https://doi.org/10.3390/toxins15030188>.
- Melo-Merino, S.M., Reyes-Bonilla, H., Lira-Noriega, A., 2020. Ecological niche models and species distribution models in marine environments: a literature review and spatial analysis of evidence. *Ecol. Model.* 415, 108837 <https://doi.org/10.1016/j.ecolmodel.2019.108837>.
- Meroni, L., Chiantore, M., Petrillo, M., Asnaghi, V., 2018. Habitat effects on *Ostreopsis* cf. *ovata* bloom dynamics. *Harmful Algae* 80, 64–71. <https://doi.org/10.1016/j.hal.2018.09.006>.
- Michelangeli, P.-A., Vrac, M., Loukos, H., 2009. Probabilistic downscaling approaches: application to wind cumulative distribution functions. *Geophys. Res. Lett.* 36, 2009GL038401 <https://doi.org/10.1029/2009GL038401>.
- Moore, S.K., Trainer, V.L., Mantua, N.J., Parker, M.S., Laws, E.A., Backer, L.C., Fleming, L.E., 2008. Impacts of climate variability and future climate change on harmful algal blooms and human health. *Environ. Health* 7, S4. <https://doi.org/10.1186/1476-069X-7-S2-S4>.
- Moullec, F., Barrier, N., Drira, S., Guilhaumon, F., Marsaleix, P., Somot, S., Ulses, C., Velez, L., Shin, Y.-J., 2019. An end-to-end model reveals losers and winners in a warming Mediterranean Sea. *Front. Mar. Sci.* 6, 345. <https://doi.org/10.3389/fmars.2019.00345>.
- Naimi, B., Hamm, N. a s, Groen, T.A., Skidmore, A.K., Toxopeus, A.G., 2014. Where is positional uncertainty a problem for species distribution modelling. *Ecography* 37, 191–203. <https://doi.org/10.1111/j.1600-0587.2013.00205.x>.
- Neves, R.A.F., Contins, M., Nascimento, S.M., 2018. Effects of the toxic benthic dinoflagellate *Ostreopsis* cf. *ovata* on fertilization and early development of the sea urchin *Lytechinus variegatus*. *Mar. Environ. Res.* 135, 11–17. <https://doi.org/10.1016/j.marenvres.2018.01.014>.
- Ninčević Gladan, Z., Arapov, J., Casabianca, S., Penna, A., Honsell, G., Brovedani, V., Pelin, M., Tartaglione, L., Sosa, S., Dell'Aversano, C., 2019. Massive occurrence of the harmful benthic dinoflagellate *Ostreopsis* cf. *ovata* in the Eastern Adriatic Sea. *Toxins* 11, 300.
- Onuma, Y., Satake, M., Ukena, T., Roux, J., Chanteau, S., Rasolofonirina, N., Ratsimaloto, M., Naoki, H., Yasumoto, T., 1999. Identification of putative palytoxin as the cause of clueteoxism. *Toxicon* 37, 55–65.
- Pages, R., Baklouti, M., Barrier, N., Ayache, M., Sevaut, F., Somot, S., Moutin, T., 2020. Projected effects of climate-induced changes in hydrodynamics on the biogeochemistry of the Mediterranean Sea under the RCP 8.5 regional climate scenario. *Front. Mar. Sci.* 7, 563615 <https://doi.org/10.3389/fmars.2020.563615>.
- Paradis, C., Chomérat, N., Vaucel, J.-A., Antajan, E., Labe, P., Rappoport, M., Labadie, M., 2024. Impacts on human health potentially caused by exposure to an unprecedented *Ostreopsis* spp bloom in the Bay of Biscay. *French Basque Coast. Wilderness Environ.* 35 (1), 13–21. <https://doi.org/10.1177/10806032231220405>.
- Pavaux, A.-S., Julie, R., Laurence, G.-G., Sophie, M., Eva, T., Thomas, O.P., Rodolphe, L., Stéphane, G., 2019. Effects of the toxic dinoflagellate *Ostreopsis* cf. *ovata* on survival, feeding and reproduction of a phycodermic copepod. *J. Exp. Mar. Biol. Ecol.* 516, 103–113. <https://doi.org/10.1016/j.jembe.2019.05.004>.
- Pavaux, A.-S., Berdalet, E., Lemée, R., 2020. Chemical ecology of the benthic dinoflagellate genus *Ostreopsis*: review of progress and future directions. *Front. Mar. Sci.* 7, 498. <https://doi.org/10.3389/fmars.2020.00498>.
- Pavaux, A.-S., Velasquez-Carjaval, D., Drouet, K., Lebrun, A., Hiroux, A., Marro, S., Christians, E., Castagnetti, S., Lemée, R., 2021. Daily variations of *Ostreopsis* cf. *ovata* abundances in NW Mediterranean Sea. *Harmful Algae* 110, 102144. <https://doi.org/10.1016/j.hal.2021.102144>.
- Penna, A., Vila, M., Fraga, S., Giacobbe, M.G., Andreoni, F., Riobó, P., Vernesi, C., 2005. Characterization of *Ostreopsis* and *Coolia* (Dinophyceae) isolates in the western mediterranean sea based on morphology, toxicity and internal transcribed spacer 5.8S rDNA sequences¹. *J. Phycol.* 41, 212–225. <https://doi.org/10.1111/j.1529-8817.2005.04011.x>.
- Pertierra, L.R., Bartlett, J.C., Duffy, G.A., Vega, G.C., Hughes, K.A., Hayward, S.A.L., Convey, P., Olalla-Tarraga, M.A., Aragón, P., 2020. Combining correlative and mechanistic niche models with human activity data to elucidate the invasive potential of a sub-Antarctic insect. *J. Biogeogr.* 47, 658–673. <https://doi.org/10.1111/jbi.13780>.
- Peterson, A.T., Papeş, M., Soberón, J., 2015. Mechanistic and correlative models of ecological niches. *Eur. J. Ecol.* 1, 28–38. <https://doi.org/10.1515/eje-2015-0014>.
- Pezzolesi, L., Guerrini, F., Ciminiello, P., Dell'Aversano, C., Iacovo, E.D., Fattorusso, E., Forino, M., Tartaglione, L., Pistocchi, R., 2012. Influence of temperature and salinity on *Ostreopsis* cf. *ovata* growth and evaluation of toxin content through HR LC-MS and biological assays. *Water Res.* 46, 82–92. <https://doi.org/10.1016/j.watres.2011.10.029>.
- Pfannkuchen, M., Godrijan, J., Marić Pfannkuchen, D., Iveša, L., Kružić, P., Ciminiello, P., Dell'Aversano, C., Dello Iacovo, E., Fattorusso, E., Forino, M., Tartaglione, L., Godrijan, M., 2012. Toxin-producing *Ostreopsis* cf. *ovata* are likely to bloom undetected along coastal areas. *Environ. Sci. Technol.* 46, 5574–5582. <https://doi.org/10.1021/es300189h>.
- Phillips, S.J., Dudík, M., Elith, J., Graham, C.H., Lehmann, A., Leathwick, J., Ferrier, S., 2009. Sample selection bias and presence-only distribution models: implications for background and pseudo-absence data. *Ecol. Appl.* 19, 181–197. <https://doi.org/10.1890/07-2153.1>.
- Pistocchi, R., Pezzolesi, L., Guerrini, F., Vanucci, S., Dell'Aversano, C., Fattorusso, E., 2011. A review on the effects of environmental conditions on growth and toxin production of *Ostreopsis ovata*. *Toxicon* 57, 421–428. <https://doi.org/10.1016/j.toxicon.2010.09.013>.
- Poloczanska, E.S., Brown, C.J., Sydeman, W.J., Kiessling, W., Schoeman, D.S., Moore, P. J., Brander, K., Bruno, J.F., Buckley, L.B., Burrows, M.T., Duarte, C.M., Halpern, B.S., Holding, J., Kappel, C.V., O'Connor, M.I., Pandolfi, J.M., Parmesan, C., Schwing, F., Thompson, S.A., Richardson, A.J., 2013. Global imprint of climate change on marine life. *Nat. Clim. Chang.* 3, 919–925. <https://doi.org/10.1038/nclimate1958>.
- Privitera, D., Giusssani, V., Isola, G., Faimali, M., Piazza, V., Garaventa, F., Asnaghi, V., Cantamessa, E., Cattaneo-Vietti, R., Chiantore, M., 2012. Toxic effects of *Ostreopsis ovata* on larvae and juveniles of *Paracentrotus lividus*. *Harmful Algae* 18, 16–23. <https://doi.org/10.1016/j.hal.2012.03.009>.
- Reimann, L., Vafeidis, A.T., Honsel, L.E., 2023. Population development as a driver of coastal risk: current trends and future pathways. *Camb. Prisms Coast. Futures* 1, e14. <https://doi.org/10.1017/cft.2023.3>.
- Robinson, L.M., Elith, J., Hobday, A.J., Pearson, R.G., Kendall, B.E., Possingham, H.P., Richardson, A.J., 2011. Pushing the limits in marine species distribution modelling: lessons from the land present challenges and opportunities: marine species distribution models. *Glob. Ecol. Biogeogr.* 20, 789–802. <https://doi.org/10.1111/j.1466-8238.2010.00636.x>.
- Robinson, N.M., Nelson, W.A., Costello, M.J., Sutherland, J.E., Lundquist, C.J., 2017. A systematic review of marine-based species distribution models (SDMs) with recommendations for best practice. *Front. Mar. Sci.* 4, 421. <https://doi.org/10.3389/fmars.2017.00421>.
- Ruti, P.M., Somot, S., Giorgi, F., Dubois, C., Flaounas, E., Obermann, A., Dell'Aquila, A., Pisacane, G., Harzallah, A., Lombardi, E., Ahrens, B., Akhtar, N., Alias, A., Arsouze, T., Aznar, R., Bastin, S., Bartholy, J., Béranger, K., Beuvier, J., Bouffies-Cloché, S., Brauch, J., Cabos, W., Calmanti, S., Calvet, J.-C., Carillo, A., Conte, D., Coppola, E., Djurdjevic, V., Drobinski, P., Elizalde-Arellano, A., Gaertner, M., Galán, P., Gallardo, C., Gualdi, S., Goncalves, M., Jorba, O., Jordá, G., L'Heveder, B., Lebeaupin-Brossier, C., Li, L., Liguori, G., Lionello, P., Maciás, D., Nabat, P., Önel, B., Raikovic, B., Ramage, K., Sevaut, F., Sannino, G., Struglia, M.V., Sanna, A., Torma, C., Vervatis, V., 2016. Med-CORDEX Initiative for Mediterranean Climate Studies. *Bull. Am. Meteorol. Soc.* 97, 1187–1208. <https://doi.org/10.1175/BAMS-D-14-00176.1>.
- Scalco, E., Brunet, C., Marino, F., Rossi, R., Soprano, V., Zingone, A., Montresor, M., 2012. Growth and toxicity responses of Mediterranean *Ostreopsis* cf. *ovata* to seasonal irradiance and temperature conditions. *Harmful Algae* 17, 25–34. <https://doi.org/10.1016/j.hal.2012.02.008>.
- Selina, M.S., Morozova, T.V., Vyshkvartsev, D.I., Orlova, T.Yu., 2014. Seasonal dynamics and spatial distribution of epiphytic dinoflagellates in Peter the Great Bay (Sea of Japan) with special emphasis on *Ostreopsis* species. *Harmful Algae* 32, 1–10. <https://doi.org/10.1016/j.hal.2013.11.005>.
- Sevaut, F., Somot, S., Alias, A., Dubois, C., Lebeaupin-Brossier, C., Nabat, P., Adloff, F., Déqué, M., Decharme, B., 2014. A fully coupled Mediterranean regional climate system model: design and evaluation of the ocean component for the 1980–2012 period. *Tellus A: Dyn. Meteorol. Oceanogr.* 66, 23967 <https://doi.org/10.3402/tellusa.v66.23967>.
- Shears, N.T., Ross, P.M., 2009. Blooms of benthic dinoflagellates of the genus *Ostreopsis*: an increasing and ecologically important phenomenon on temperate reefs in New Zealand and worldwide. *Harmful Algae* 8, 916–925. <https://doi.org/10.1016/j.hal.2009.05.003>.
- Soberón, J., Peterson, A.T., 2005. Interpretation of models of fundamental ecological niches and species' distributional areas. *Biodivers. Inform.* 2, 1–10. <https://doi.org/10.17161/bi.v2i04>.
- Soto-Navarro, J., Jordá, G., Amores, A., Cabos, W., Somot, S., Sevaut, F., Maciás, D., Djurdjevic, V., Sannino, G., Li, L., Sein, D., 2020. Evolution of Mediterranean Sea water properties under climate change scenarios in the Med-CORDEX ensemble. *Clim. Dyn.* 54, 2135–2165. <https://doi.org/10.1007/s00382-019-05105-4>.
- Tester, P.A., Litaker, R.W., Berdalet, E., 2020. Climate change and harmful benthic microalgae. *Harmful Algae* 91, 101655. <https://doi.org/10.1016/j.hal.2019.101655>.
- Thomas, Y., Bacher, C., 2018. Assessing the sensitivity of bivalve populations to global warming using an individual-based modelling approach. *Glob. Chang. Biol.* 24, 4581–4597. <https://doi.org/10.1111/gcb.14402>.
- Tichadou, L., Glaizal, M., Armengaud, A., Grosseil, H., Lemée, R., Kantin, R., Lasalle, J.-L., Drouet, G., Rambaud, L., Malfait, P., 2010. Health impact of unicellular algae of the *Ostreopsis* genus blooms in the Mediterranean Sea: experience of the French Mediterranean coast surveillance network from 2006 to 2009. *Clin. Toxicol.* 48, 839–844.
- Totti, C., Accoroni, S., Cerino, F., Cucchiari, E., Romagnoli, T., 2010. *Ostreopsis ovata* bloom along the Conero Riviera (northern Adriatic Sea): relationships with environmental conditions and substrata. *Harmful Algae* 9, 233–239. <https://doi.org/10.1016/j.hal.2009.10.006>.
- Trainer, V.L., 2020. GlobalHAB: Evaluating, Reducing and Mitigating the Cost of Harmful Algal Blooms: A Compendium of Case Studies. North Pacific Marine Science Organization.

- Tubaro, A., Durando, P., Del Favero, G., Ansaldi, F., Icardi, G., Deeds, J.R., Sosa, S., 2011. Case definitions for human poisonings postulated to palytoxins exposure. *Toxicon* 57, 478–495. <https://doi.org/10.1016/j.toxicon.2011.01.005>.
- Ulses, C., Estournel, C., Fourier, M., Coppola, L., Kessouri, F., Lefèvre, D., Marsaleix, P., 2021. Oxygen budget of the north-western Mediterranean deep- convection region. *Biogeosciences* 18, 937–960. <https://doi.org/10.5194/bg-18-937-2021>.
- Vila, M., Garcés, E., Masó, M., 2001. Potentially toxic epiphytic dinoflagellate assemblages on macroalgae in the NW Mediterranean. *Aquat. Microb. Ecol.* 26, 51–60. <https://doi.org/10.3354/ame026051>.
- Vila, M., Masó, M., Sampedro, N., Illoul, H., Arin, L., Garcés, E., Giacobbe, M.G., Alvarez, J., Camp, J., 2008. The genus *Ostreopsis* in recreational waters of the Catalan Coast and Balearic Islands (NW Mediterranean Sea): is this the origin of human respiratory difficulties. In: *Proceedings of the 12th International Conference on Harmful Algae. International Society for the Study of Harmful Algae and Intergovernmental ...*, pp. 334–336.
- Vila, M., Arin, L., Battocchi, C., Bravo, I., Fraga, S., Penna, A., Reñé, A., Riobó, P., Rodríguez, F., Sala, M.M., Camp, J., Torres, M.D., Franco, J.M., 2012. Management of *Ostreopsis* Blooms in recreational waters along the Catalan coast (NW Mediterranean Sea): cooperation between a research project and a monitoring program. *Cryptogam. Algal.* 33, 143–152. <https://doi.org/10.7872/crya.v33.iss2.2011.143>.
- Vila, M., Abós-Herrándiz, R., Isern-Fontanet, J., Álvarez, J., Berdalet, E., 2016. Establishing the link between *Ostreopsis* cf. *ovata* blooms and human health impacts using ecology and epidemiology. *Sci. Mar.* 80, 107–115. <https://doi.org/10.3989/scimar.04395.08A>.
- Vrac, M., Michelangeli, P.-A., 2015. Package ‘CDFT’ [WWW Document]. URL: <https://cran.r-project.org/web/packages/CDFT/index.html>.
- Voltaire, A., Sanchez-Gomez, E., Salas, Y., Méliá, D., Decharme, B., Cassou, C., Sénési, S., Valcke, S., Beau, I., Alias, A., Chevallier, M., Déqué, M., Deshayes, J., Douville, H., Fernandez, E., Madec, G., Maisonnave, E., Moine, M.-P., Planton, S., Saint-Martin, D., Szopa, S., Tyteca, S., Alkama, R., Belamari, S., Braun, A., Coquart, L., Chauvin, F., 2013. The CNRM-CM5.1 global climate model: description and basic evaluation. *Clim. Dyn.* 40, 2091–2121. <https://doi.org/10.1007/s00382-011-1259-y>.
- Vrac, M., Drobinski, P., Merlo, A., Herrmann, M., Lavaysse, C., Li, L., Somot, S., 2012. Dynamical and statistical downscaling of the French Mediterranean climate: uncertainty assessment. *Nat. Hazards Earth Syst. Sci.* 12, 2769–2784. <https://doi.org/10.5194/nhess-12-2769-2012>.
- Wei, T., Simko, V., 2021. R package “corrplot”: Visualization of a Correlation Matrix [WWW Document]. URL: <https://github.com/taiyun/corrplot>.
- Wittmann, A.C., Pörtner, H.-O., 2013. Sensitivities of extant animal taxa to ocean acidification. *Nat. Clim. Chang.* 3, 995–1001. <https://doi.org/10.1038/nclimate1982>.
- Yates, K.L., Bouchet, P.J., Caley, M.J., Mengersen, K., Randin, C.F., Parnell, S., Fielding, A.H., Bamford, A.J., Ban, S., Barbosa, A.M., Dormann, C.F., Elith, J., Embling, C.B., Ervin, G.N., Fisher, R., Gould, S., Graf, R.F., Gregr, E.J., Halpin, P.N., Heikkinen, R.K., Heinänen, S., Jones, A.R., Krishnakumar, P.K., Lauria, V., Lozano-Montes, H., Mannocci, L., Mellin, C., Mesgaran, M.B., Moreno-Amat, E., Mormede, S., Novaczek, E., Oppel, S., Ortuño Crespo, G., Peterson, A.T., Rapacciolo, G., Roberts, J.J., Ross, R.E., Scales, K.L., Schoeman, D., Snelgrove, P., Sundblad, G., Thuiller, W., Torres, L.G., Verbruggen, H., Wang, L., Wenger, S., Whittingham, M.J., Zharikov, Y., Zurell, D., Sequeira, A.M.M., 2018. Outstanding challenges in the transferability of ecological models. *Trends Ecol. Evol.* 33, 790–802. <https://doi.org/10.1016/j.tree.2018.08.001>.
- Zingone, A., Siano, R., D’Alelio, D., Sarno, D., 2006. Potentially toxic and harmful microalgae from coastal waters of the Campania region (Tyrrhenian Sea, Mediterranean Sea). *Harmful Algae* 5, 321–337. <https://doi.org/10.1016/j.hal.2005.09.002>.
- Zingone, A., Escalera, L., Aligizaki, K., Fernández-Tejedor, M., Ismael, A., Montresor, M., Mozetič, P., Taş, S., Totti, C., 2021. Toxic marine microalgae and noxious blooms in the Mediterranean Sea: a contribution to the Global HAB Status Report. *Harmful Algae* 102, 101843. <https://doi.org/10.1016/j.hal.2020.101843>.